Supplementary Information

Picolinate-Based Acyclic Ligand for Rare Earth Element Extraction and Separation

Yangyang Gao[1,2], Sean Medin[3], Alexa M. Schmitz[3], Justin J. Wilson[1,2]

[1] Department of Chemistry and Biochemistry
University of California Santa Barbara, Santa Barbara, California 93106, United States

[2] Department of Chemistry and Chemical Biology
Cornell University, Ithaca, New York 14853, United States

[3] REEgen Inc., Ithaca, New York 14853, United States

Table of Contents

S1. Ligand synthesis

S1.1 General consideration

All reagents and solvents were obtained commercially and used without further purification unless otherwise noted. Deionized H_2O was obtained from an Elga Purelab Flex 2 water purification system with an electrical resistivity $\geqslant$18.2 MΩ·cm. Lanthanide chloride salts were of trace metal grade (99.9%). Organic solvents were of ACS grade or higher, and solvents noted as dry were obtained following storage over activated 3 Å molecular sieves.

HPLC

High-performance liquid chromatography (HPLC) used in this study was equipped with an LC-20AP (preparative) or LC-20AT (analytical) pump, and an SPD-20AV UV−vis detector monitoring at 270 nm and 220 nm (Shimadzu, Japan). Analytical chromatography was carried out using an Ultra Aqueous C18 column (100 Å, 5 μm, 250 mm × 4.6 mm, Restek, Bellefonte, PA) at a flow rate of 1.0 mL/min. Semipreparative purification was performed using an Epic Polar preparative column (120 Å, 10 μm, 25 cm × 20 mm, ES Industries) at a flow rate of 14 mL/min. All HPLC methods employed use a binary mobile phase. Analytical HPLC (method 1) was carried out with the method: 0−5 min, 10% MeOH/H_2O; 5−25 min, 10% → 100% MeOH/H_2O; 25−30 min, 100% → 10% MeOH/H_2O; Preparative HPLC (method 2) were carried out with the method: 0−5 min, 10% MeOH/H_2O; 5−25 min, 10% → 100% MeOH/H_2O; 25−30 min, 100% → 10% MeOH/H_2O.

LC-MS

Liquid Chromatography-Mass Spectrometry (LC-MS) used in this study was equipped with an LC-2060C 3D (analytical) pump, and a LC-MS2050 mass spectrum, and an SPD-20AV UV-vis detector monitoring at 254 nm and 220 nm (Shimadzu, Japan). Analytical chromatography was carried out using an ultra Aqueous Nexcol C18 column (100 Å, 1.8 μm, 50 mm × 2.1 mm, Shimadzu, Japan) at a flow rate of 1.0 mL/min.

NMR spectra

NMR spectra were performed at 25 °C on a 500 MHz Bruker AVIII HD spectrometer equipped with a 5 mm, broadband prodigy cryoprobe at 500 MHz and 126 MHz for ^{1}H and ^{13}C observations, respectively. Chemical shifts are reported in parts per million (ppm). ^{1}H NMR and $^{13}C\{^{1}H\}$ NMR peaks were referenced to TMS internal standard (δ = 0 ppm) or to the residual solvent signal (marked with an asterisk in the spectra). Spectra acquired in D_2O were spiked 1,4-dioxane or acetonitrile as an internal reference (^{1}H NMR δ = 3.74 ppm for 1,4-dioxane and 2.05 ppm for acetonitrile, $^{13}C\{^{1}H\}$ NMR δ = 67.15 ppm for 1,4-dioxane and 118.3 ppm for acetonitrile).

UV-vis and elemental analysis

UV-vis spectra were collected using 1 cm quartz cuvettes (3.5 mL) on a Shimadzu UV-1900 spectrometer (Shimadzu, Kyoto, Japan), and elemental analyses (C, H, N mode) were performed by Atlantic Microlab, Inc. (Norcross, GA).

Inductively coupled plasma optical emission spectroscopy (ICP-OES)

Inductively coupled plasma optical emission spectroscopy (ICP-OES) was performed on a PerkinElmer Avio 220 Max ICP-OES (PerkinElmer, Shelton Ct, US). High purity argon is used as the ICP torch gas and air is used for the optical purge gas. The plasma torch position was adjusted

by a dual-viewing optics (radial and axial) aligning with Mn (1 ppm) solution. ICP standard solutions of the mixed REEs and non-REEs (~10 µg/mL) in nitric acid were purchased from VWR (BDH Aristar) to make a calibration curve. All samples and calibration standards were acidified using 2% (v/v) HNO_3. Samples for ICP-OES were made by diluting each aqueous phase (50 µL) with 2% HNO_3 to a final volume of 5 mL The intensity of the metal ions was measured at the following wavelength all in units of nm: La: 398.852, Lu: 261.542, Ce: 413.764, Pr: 390.844, Nd: 406.109, Gd: 376.839, Tb:350.917, Dy:353.170, Yb 328.937, Cu 327.393: Ni:231.604, Zn:206.200, Ba:233.527, Mg:285.213, Al: 396.153, Ca: 317.933, Fe: 238.204; Sr: 407.771. Blank and calibration standards were re-analyzed periodically to check for sample carryover and loss of calibration, respectively.

Methyl 6-formylpicolinate **(1)** was synthesized with a previously reported method.[1]

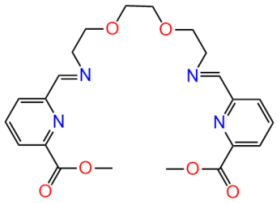

Dimethyl 6,6'-((1E,11E)-5,8-dioxa-2,11-diazadodeca-1,11-diene-1,12-diyl)dipicolinate (2). 2,2'-(ethylenedioxy)bis(ethylamine) (1 g, 6.75 mmol) was dissolved in 20 mL methanol and added dropwise to a solution of **(1)** (2.22 g, 13.5 mmol) in boiling methanol (80 mL). The resulting solution was heated at 80 °C for 1 h. After cooling down to room temperature, the yellow solution was filtered and the solvent was removed by rotary evaporation to give a yellow residue, which was suspended in 100 mL diethyl ether and stored at 4 °C overnight to give a white powder (2.70 g, 6.11 mmol). Yield: 90.5%. ^{1}H NMR (500 MHz, $CDCl_3$) δ 8.54 (q, J = 1.3 Hz, 2H, CH=N), 8.25 (d, J = 7.9, 2*H*, Ar-H), 8.17 (d, J = 7.9, 2*H*, Ar-H), 7.91 (t, J = 7.8, 0.7 Hz, 2H, Ar-H), 4.05 (s, 6H, CH_3-O), 3.88 (tt, J = 5.2, 1.2 Hz, 4H, CH_2O), 3.82 (ddd, J = 6.4, 5.2, 0.9 Hz, 4H, CH_2O), 3.66 (s, 4H, CH_2N). $^{13}C\{^{1}H\}$ NMR (126 MHz, $CDCl_3$) δ 165.51, 163.05, 154.87, 147.62, 137.57, 126.22, 124.31, 70.61, 70.51, 60.77, 53.08.

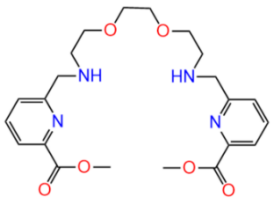

Dimethyl 6,6'-(5,8-dioxa-2,11-diazadodecane-1,12-diyl)dipicolinate (3). Compound **2** (2.5 g, 5.66 mmol) was dissolved in 60 mL methanol and cooled in ice bath. To this solution was added $NaBH_4$ (251 mg, 6.63 mmol) in portions during stirring. The resulting yellow solution was stirred on ice for 2 h. The dark red precipitate formed was removed by filtration, and the filtrate was poured into 100 mL saturated $NaHCO_3$ aqueous solution. The methanol in the resulting suspension was removed by rotary evaporation, and the remaining material was extracted with 3 × 50 mL of DCM. The organic layers were combined and dried over Na_2SO_4 and evaporated to give compound **3** as a yellow oil, which was used for next step without further purification. Yield: 2.36 g (93.7%) ^{1}H NMR (500 MHz, $CDCl_3$) δ 8.00 (dd, *J* = 7.7, 1.0 Hz, 2H, Ar-H), 7.80 (t, *J* = 7.8 Hz, 2H, Ar-H), 7.62 (dd, *J* = 7.8, 1.0 Hz, 2H, Ar-H), 4.05 (s, 4H, Ar-CH_2), 3.99 (s, 6H, CH_3O), 3.68 – 3.58 (m, 8H, CH_2O), 2.86 (q, *J* = 4.6 Hz, 4H, CH_2N).

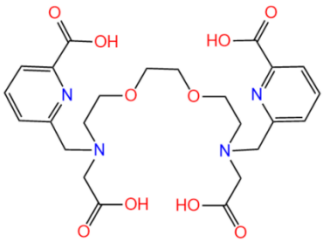

Dimethyl 3,12-bis((6-(methoxycarbonyl)pyridin-2-yl)methyl)-6,9-dioxa-3,12-diazatetradecanedioate (H_4aapa. Compound **3** and 3.26 g Na_2CO_3 (30.75 mmol) were dissolved in 40 mL acetonitrile and stirred at 80 °C for 30 min. To this boiling suspension was added bromoacetate (940 µL, 10.24 mmol), and the mixture was allowed to stir for 16 h. After cooling to room temperature, the reaction mixture was filtered, and the filtrate was concentrated to dryness by rotary evaporation to give a yellow residue, which was dissolved in 6 M HCl (15 mL) and heated at 90 °C overnight. The volatiles were removed under reduced pressure, and the residue was purified by prep-HPLC (Method 1). Analytically pure fractions were combined and evaporated to dryness. The residue was dissolved twice in 6 M HCl (15 mL) and evaporated to dryness by rotary evaporator to remove residual TFA. The H_4aapa•4HCl•5H_2O solid obtained was dissolved in water (10 mL) and dried under vacuum in a lyophilizer for 1 d. Yield: (1.91 g, 51.0%) ^{1}H NMR (500 MHz, D_2O) δ 7.85 (t, *J* = 7.7 Hz, 2H, Ar-H), 7.78 (dd, *J* = 7.7, 1.1 Hz, 2H, Ar-H), 7.54 (dd, *J* = 7.6, 1.2 Hz, 2H, Ar-H), 3.96 (s, 4H, CH_2-Ar), 3.56 (t, *J* = 5.7 Hz, 4H, CH_2O), 3.46 (s, 4H, CH_2O), 3.27 (s, 4H, CH_2O), 2.86 (t, *J* = 5.5 Hz, 4H, CH_2N), 2.21 (s, 4H, CH_2O). $^{13}C\{^{1}H\}$ NMR (126 MHz, D_2O) δ 179.26, 173.17, 158.01, 152.94, 138.30, 125.61, 122.26, 69.20, 68.18, 66.61, 59.92, 58.48, 53.11, 48.90. Elemental Analysis Calcd for $C_{24}H_{30}N_4O_{10}$·4HCl·5H_2O. C 37.49; H 5.46; N 7.28. Found C 36.98; H 5.63; N 7.09. m/z = 535.0 ($[M + H]^+$, Calcd: 535.2), t_R = 14.94 min.

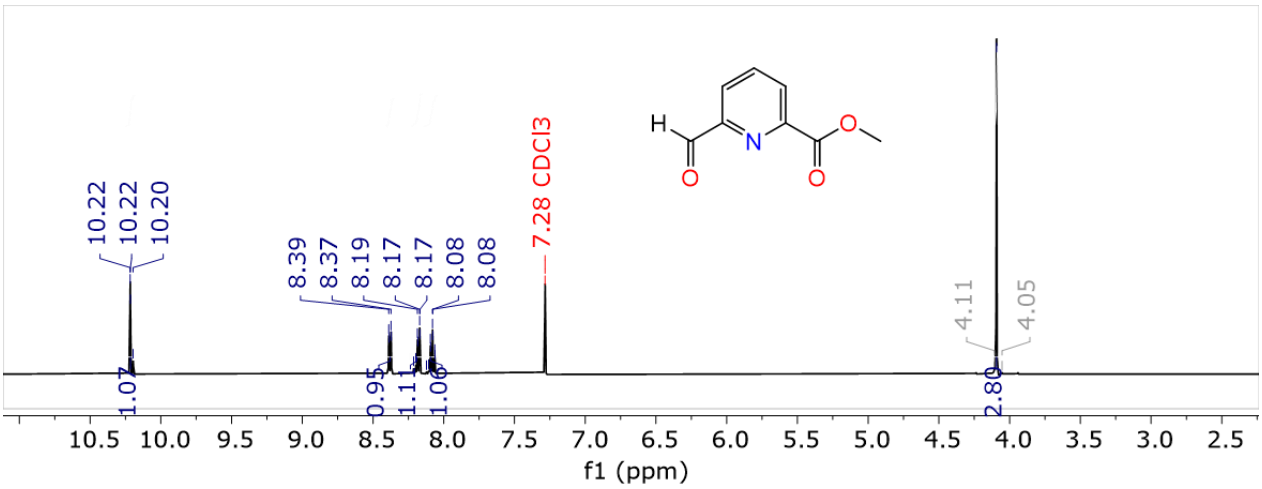

Figure S1. ^{1}H NMR spectrum of **1** (126 MHz, $CDCl_3$, 25 °C).

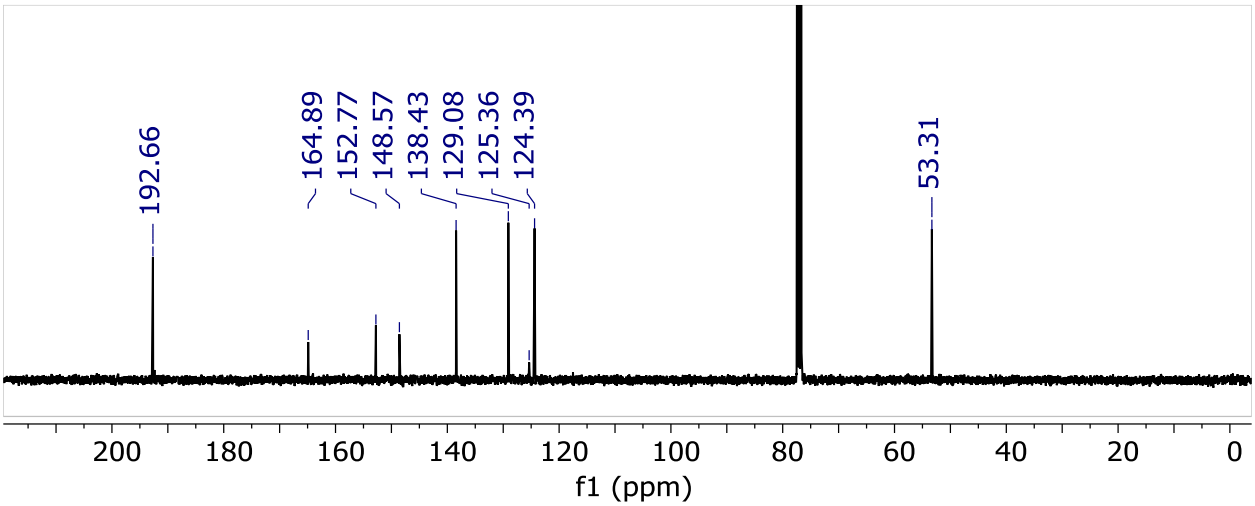

Figure S2. $^{13}C\{^{1}H\}$ NMR spectrum of **1** (126 MHz, $CDCl_3$, 25 °C).

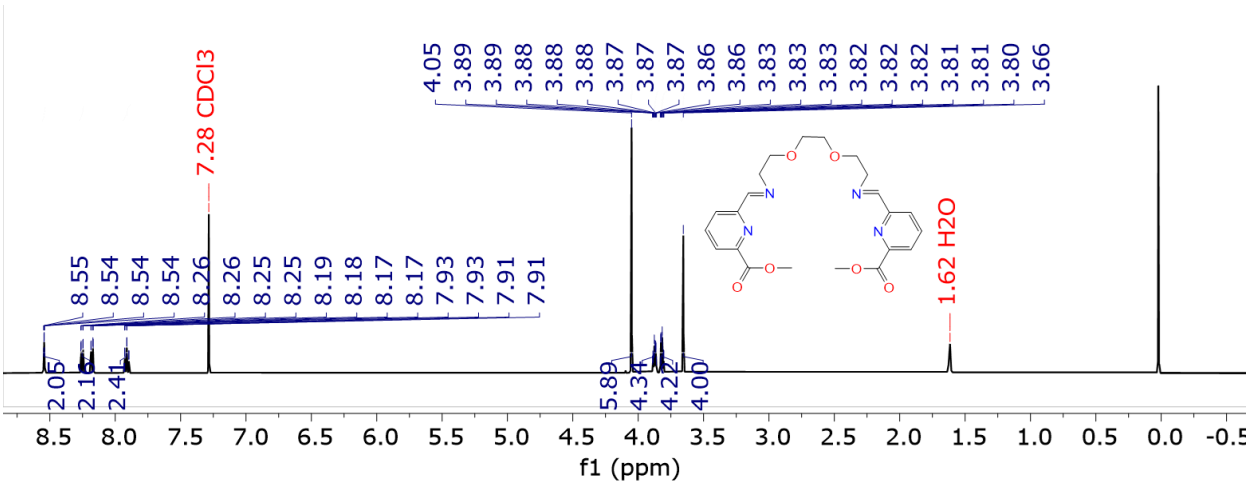

Figure S3. ^{1}H NMR spectrum of **2** (126 MHz, $CDCl_3$, 25 °C).

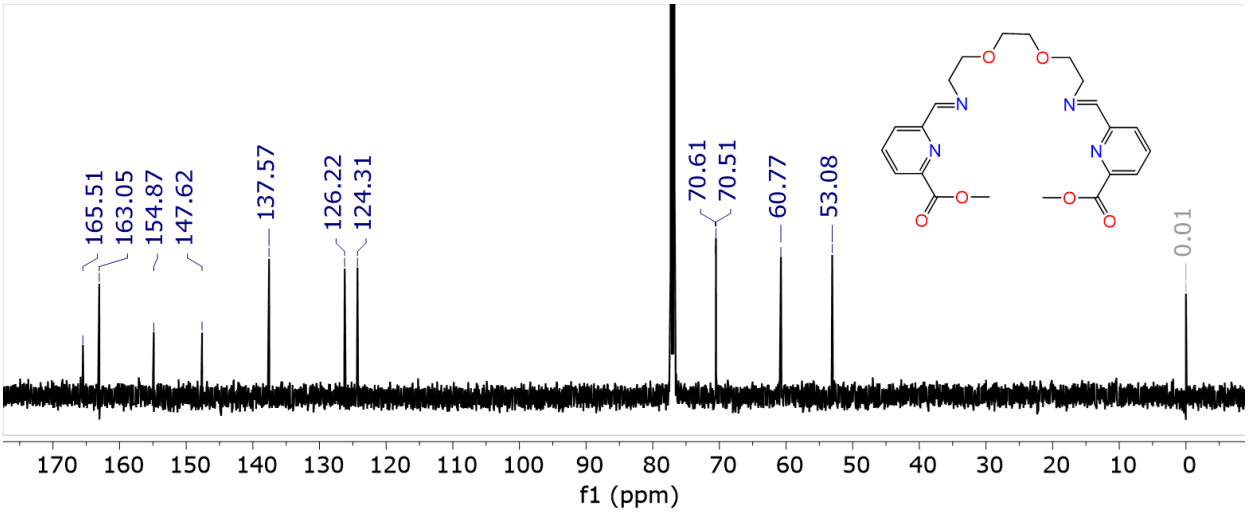

Figure S4. $^{13}C\{^{1}H\}$ NMR spectrum of **2** (126 MHz, $CDCl_3$, 25 °C).

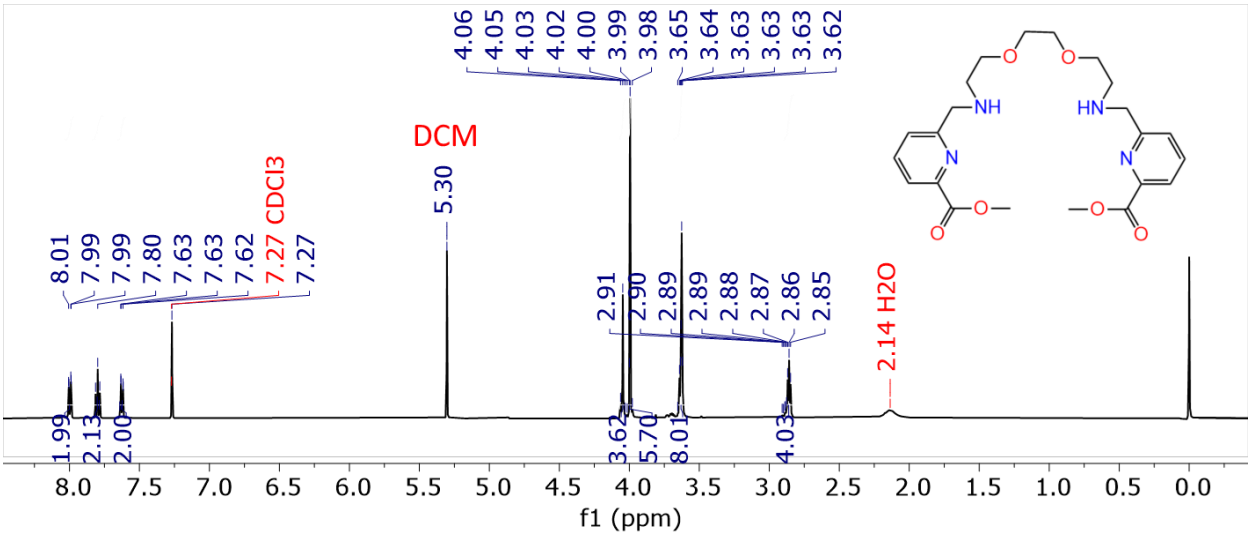

Figure S5. ^{1}H NMR spectrum of **3** (500 MHz, $CDCl_3$, 25 °C).

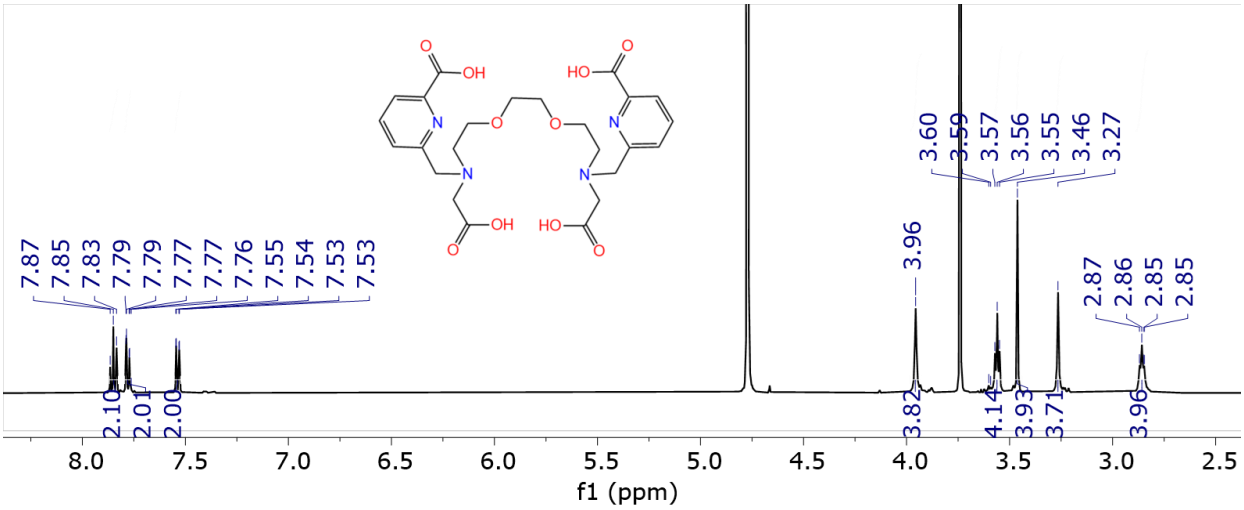

Figure S6. ^{1}H NMR spectrum of **H$_4$aapa** (500 MHz, pD = 8, D_2O, 25 °C). Dioxane was added as internal reference.

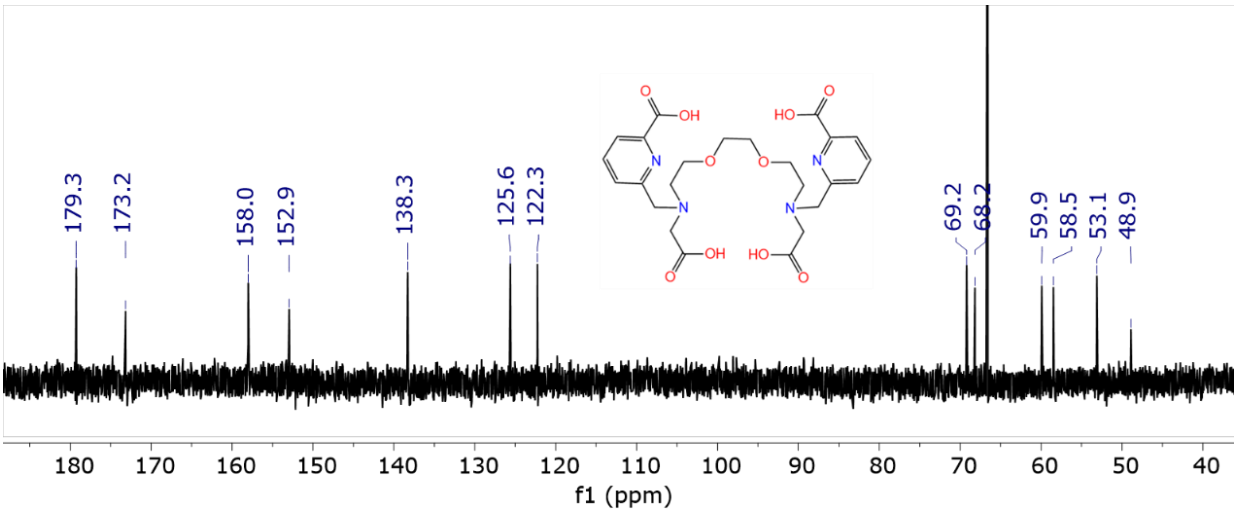

Figure S7. $^{13}C\{^{1}H\}$ NMR spectrum of **H$_4$aapa** (126 MHz, pD = 8, D_2O, 25 °C). Dioxane was added as internal reference.

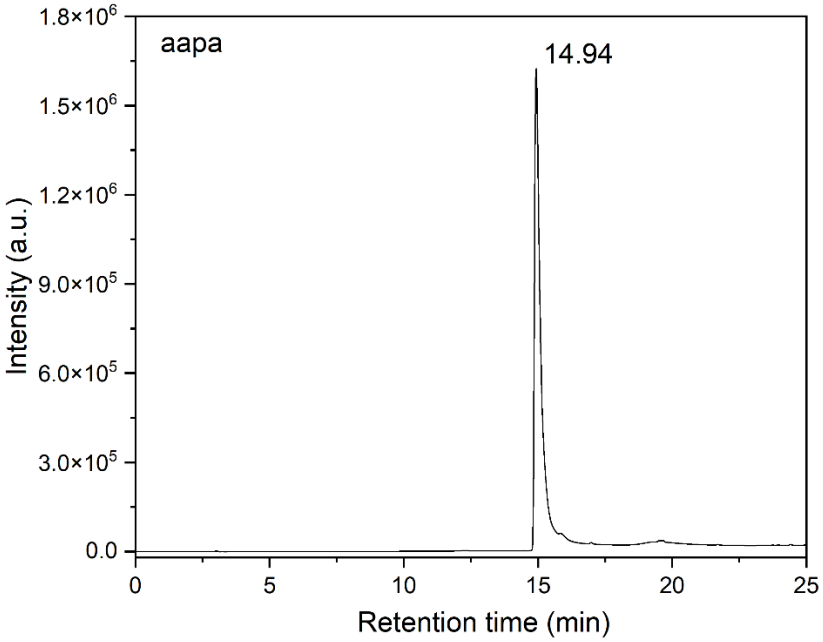

Figure S8. HPLC chromatogram of H_4aapa (Method: quick-MeOH, 270 nm detector).

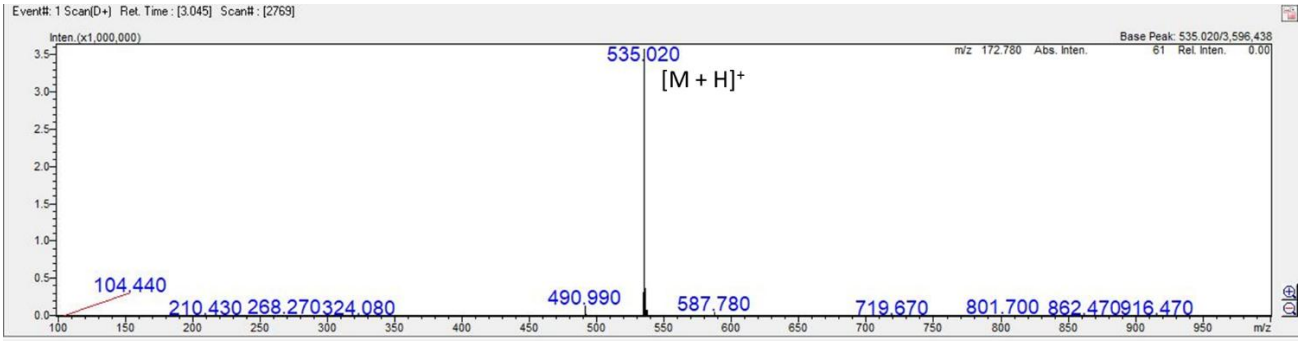

Figure S9. MS of H_4aapa.

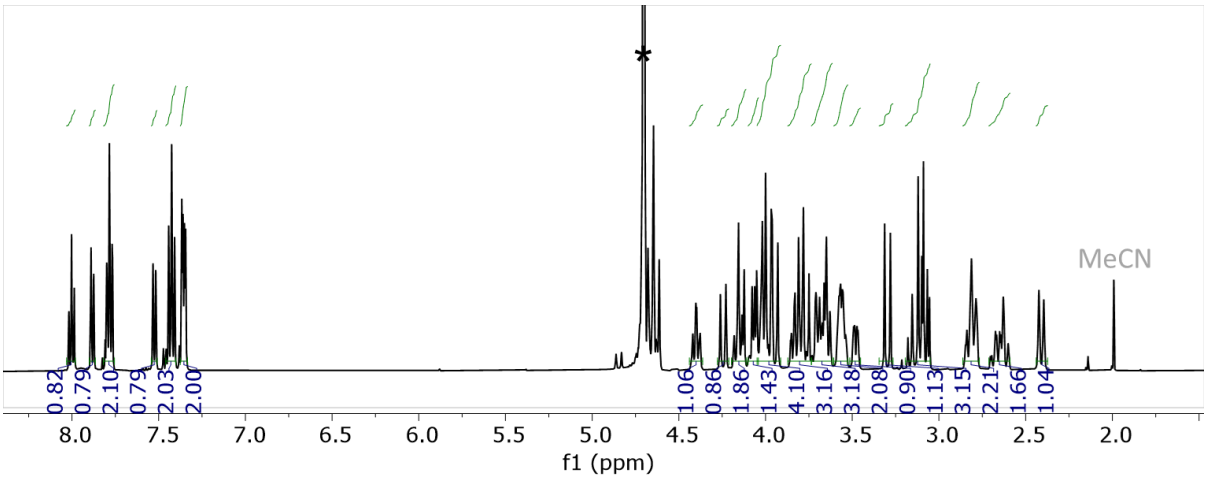

Figure S10. ^{1}H NMR spectrum of the aapa complex formed with La^{3+} (500 MHz, D_2O*, pD = 8, 25 ˚C). MeCN was added as internal reference.

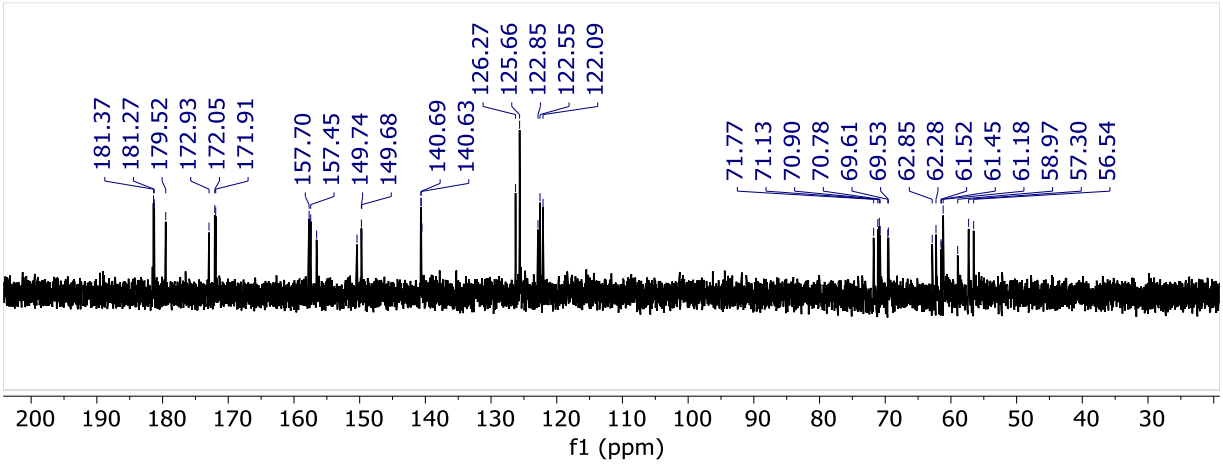

Figure S11. $^{13}C\{^{1}H\}$ NMR spectrum of the aapa complex formed with La^{3+} (126 MHz, D_2O, pD = 8, 25 ˚C). MeCN was added as internal reference.

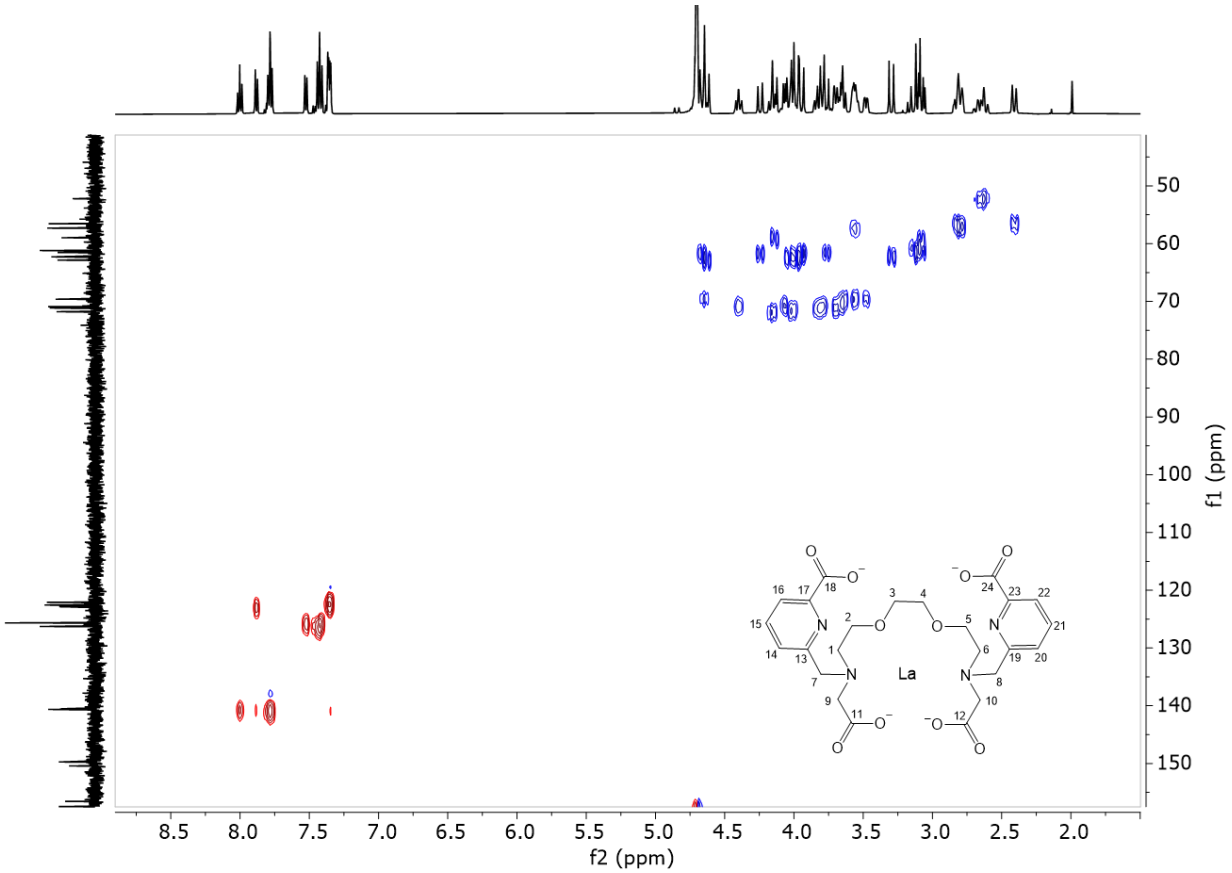

Figure S12. Full ^{1}H-^{13}C HSQC NMR spectrum of 1:1 aapa and La^{3+} mixture (500 MHz, D_2O, pD = 8, 25 °C). Acetonitrile was added as an internal reference.

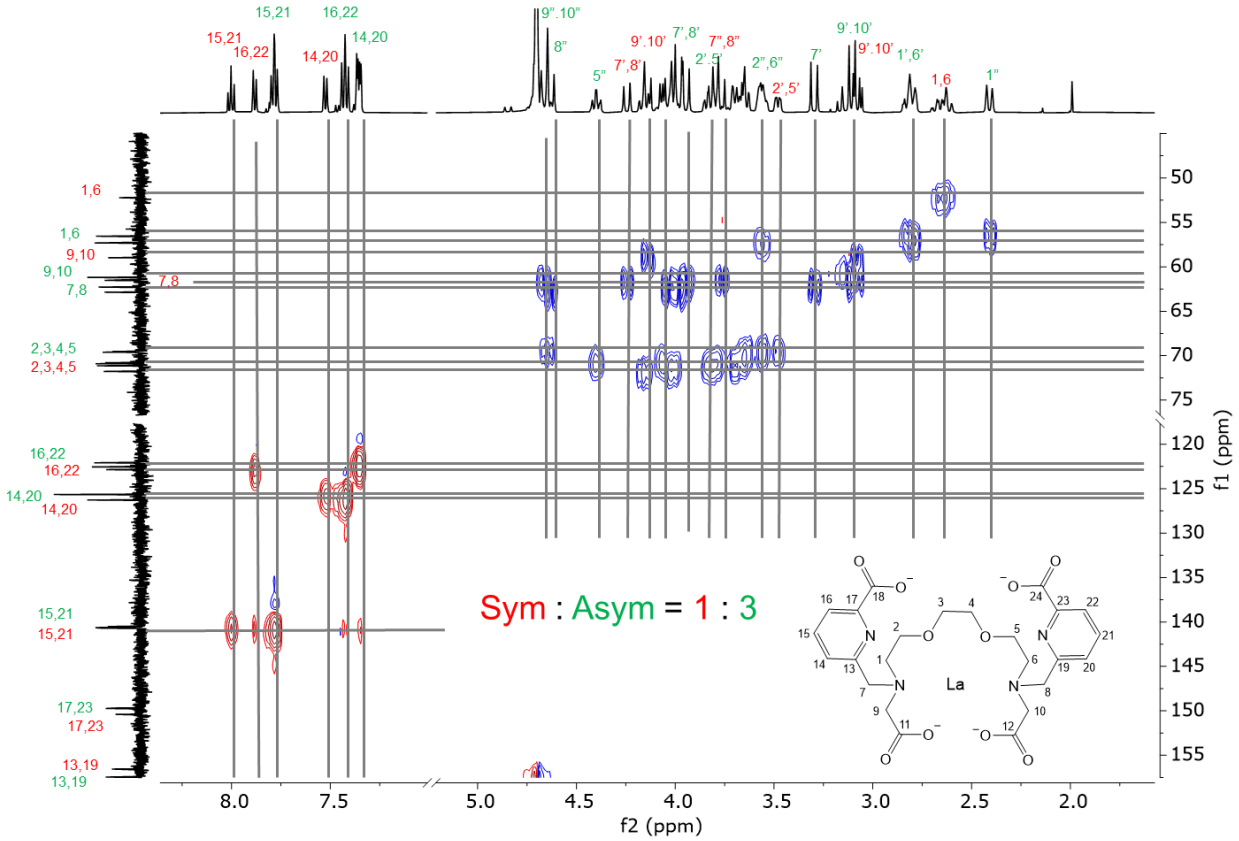

Figure S13. Truncated and assigned ^{1}H-^{13}C HSQC NMR spectrum of a 1:1 aapa:La^{3+} mixture (500 MHz, D_2O, pD = 8, 25 °C). Acetonitrile was added as an internal reference.

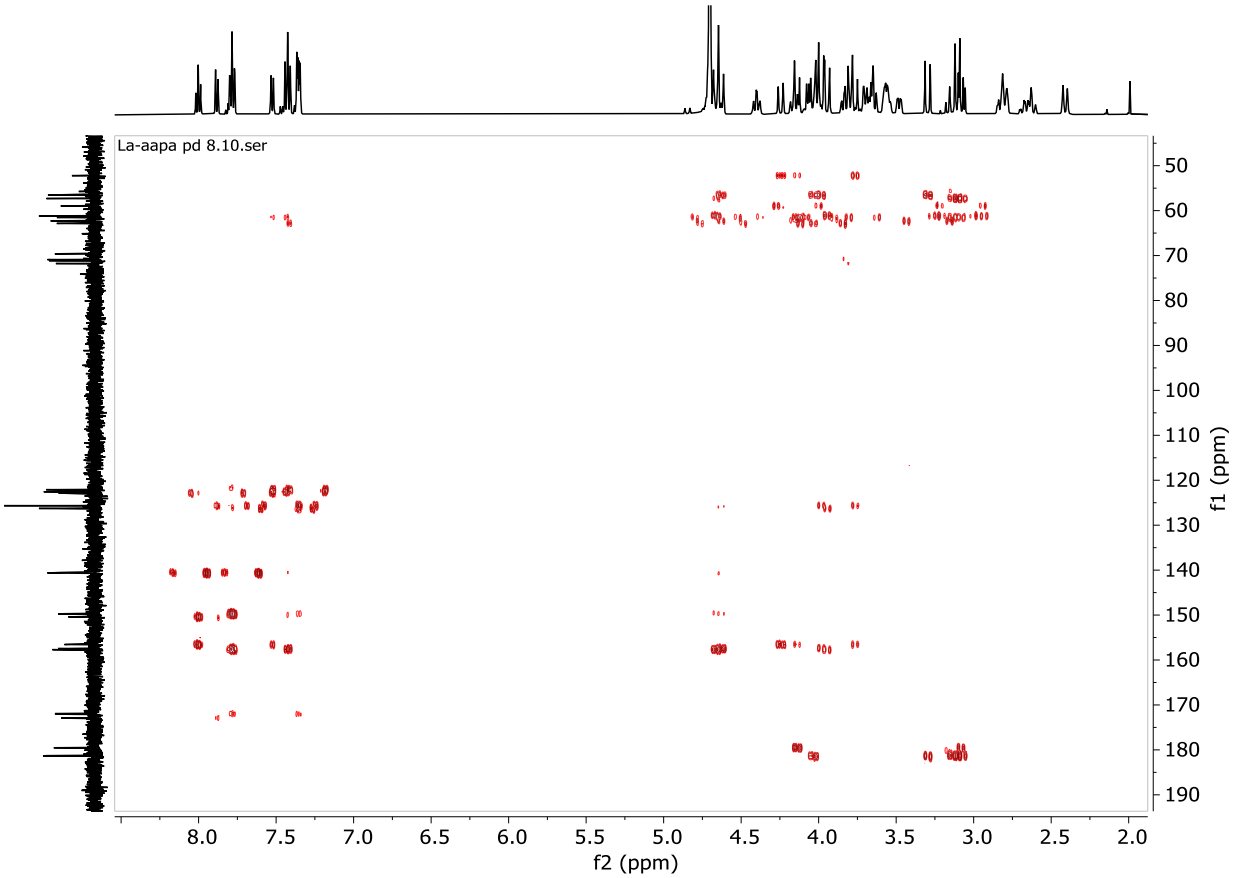

Figure S14. Full ^{1}H-^{13}C HMBC NMR spectrum of a 1:1 aapa:La^{3+} mixture (500 MHz, D_2O, pD = 8, 25 °C). Acetonitrile was added as an internal reference.

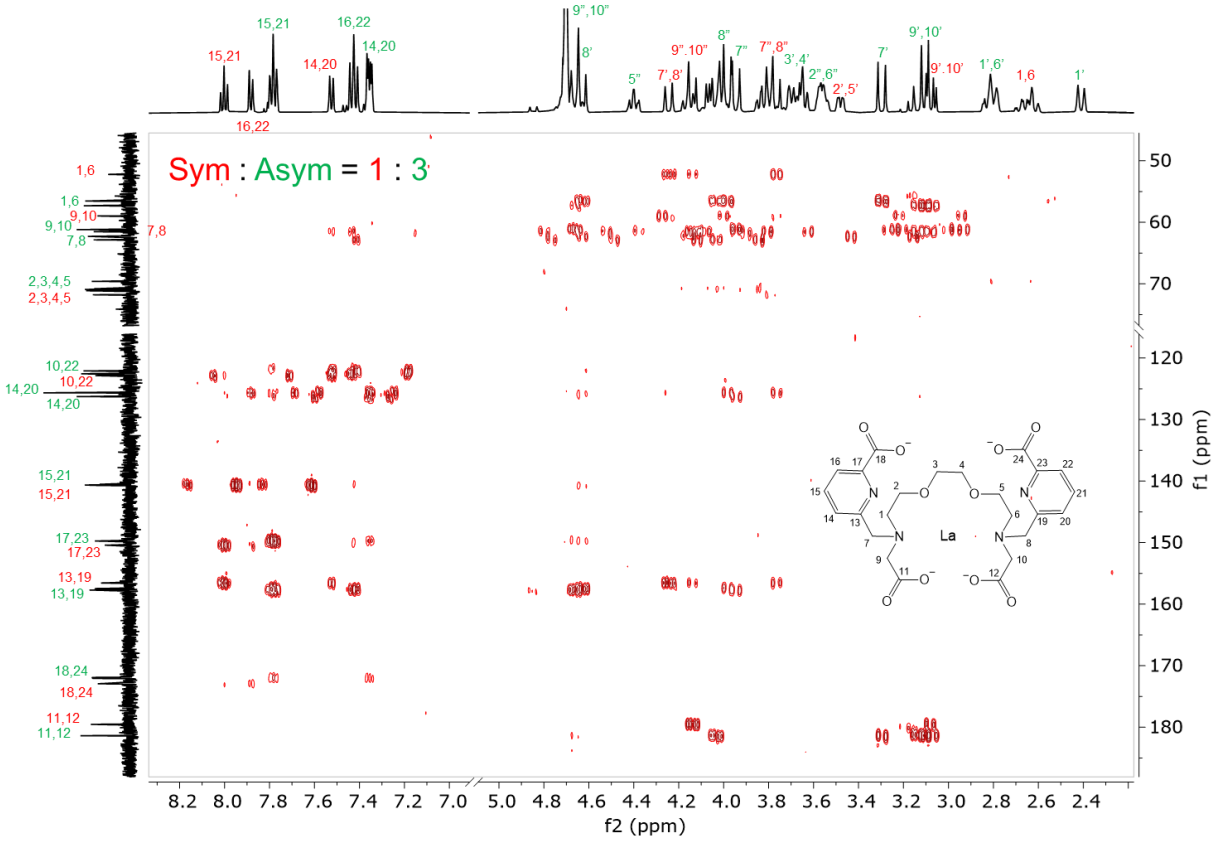

Figure S15. Truncated and labeled ^{1}H-^{13}C HMBC NMR spectrum of 1:1 aapa:La^{3+} mixture (500 MHz, D_2O, pD = 8, 25 °C). Acetonitrile was added as an internal reference.

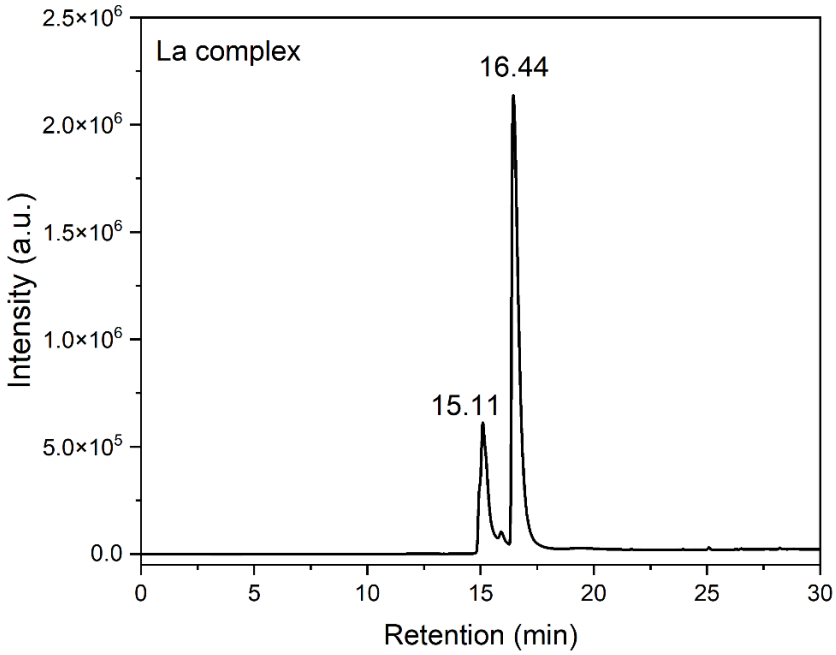

Figure S16. HPLC chromatogram of 1:1 mixture of La^{3+} and aapa (Method quick-MeOH, 270 nm detector).

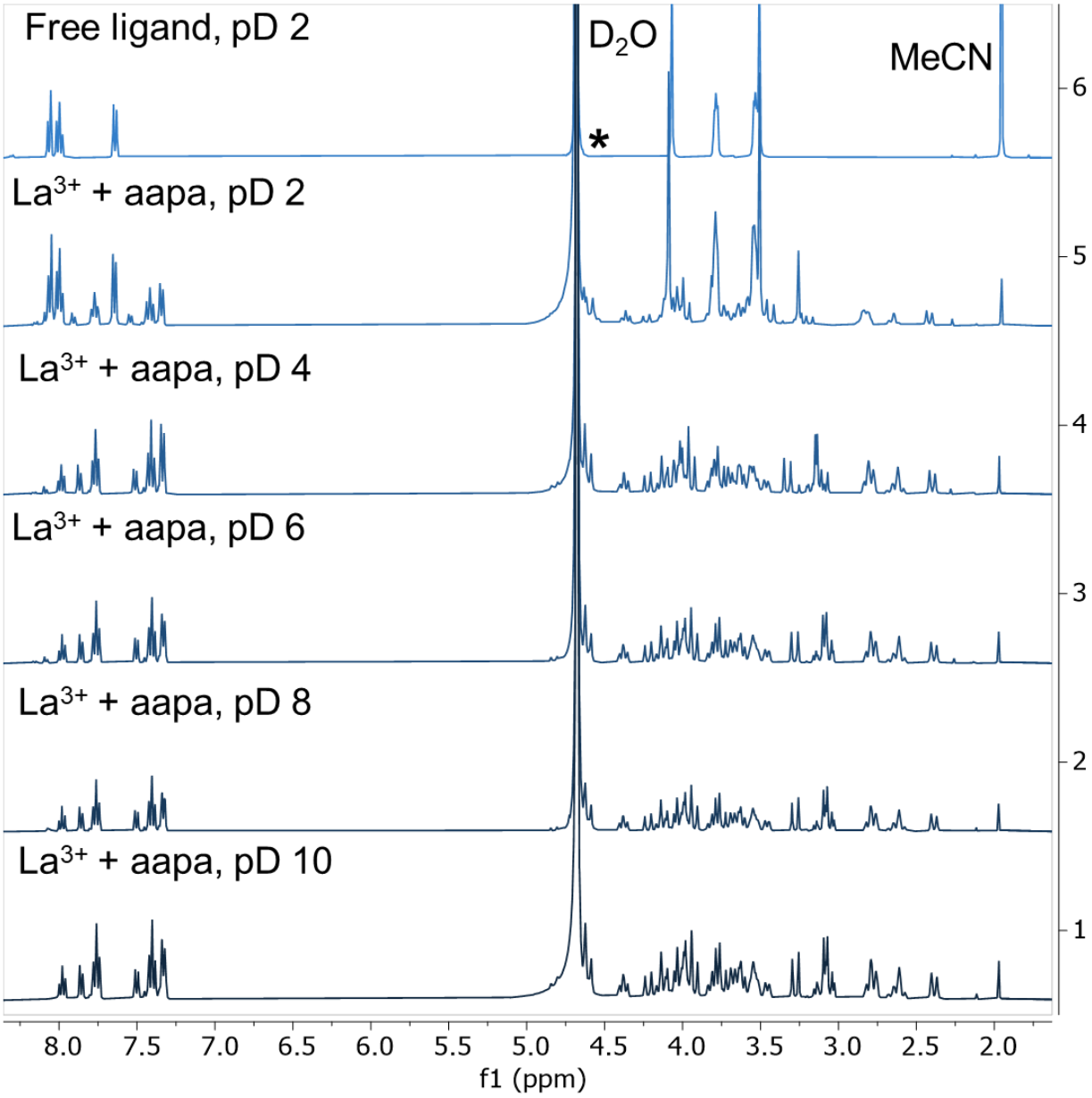

Figure S17. ^{1}H NMR spectra of free ligand and a 1:1 mixture of La^{3+} and aapa at different pD values.

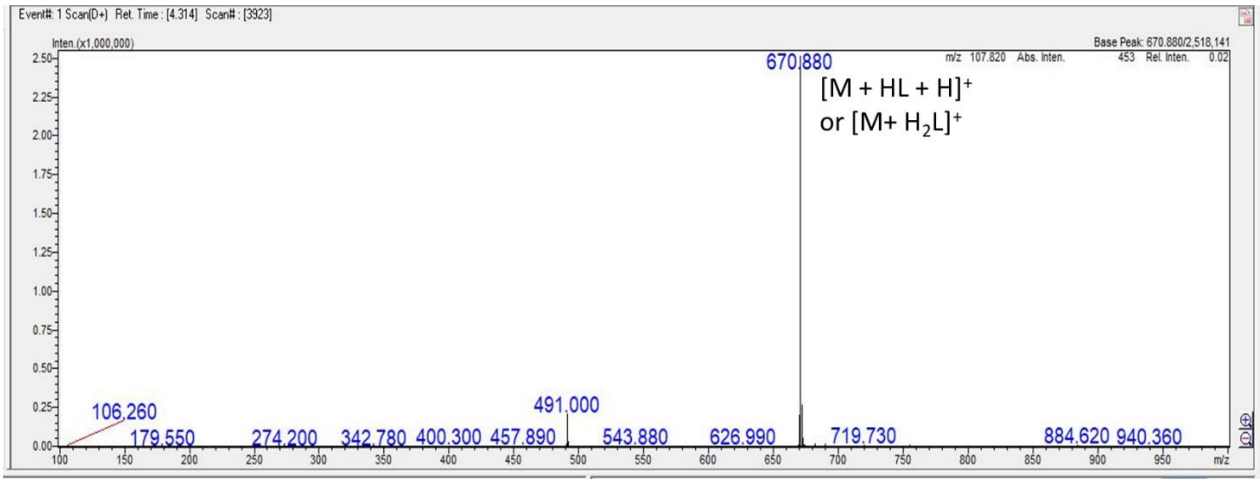

Figure S18. MS of 1:1 mixture of La^{3+} and aapa .

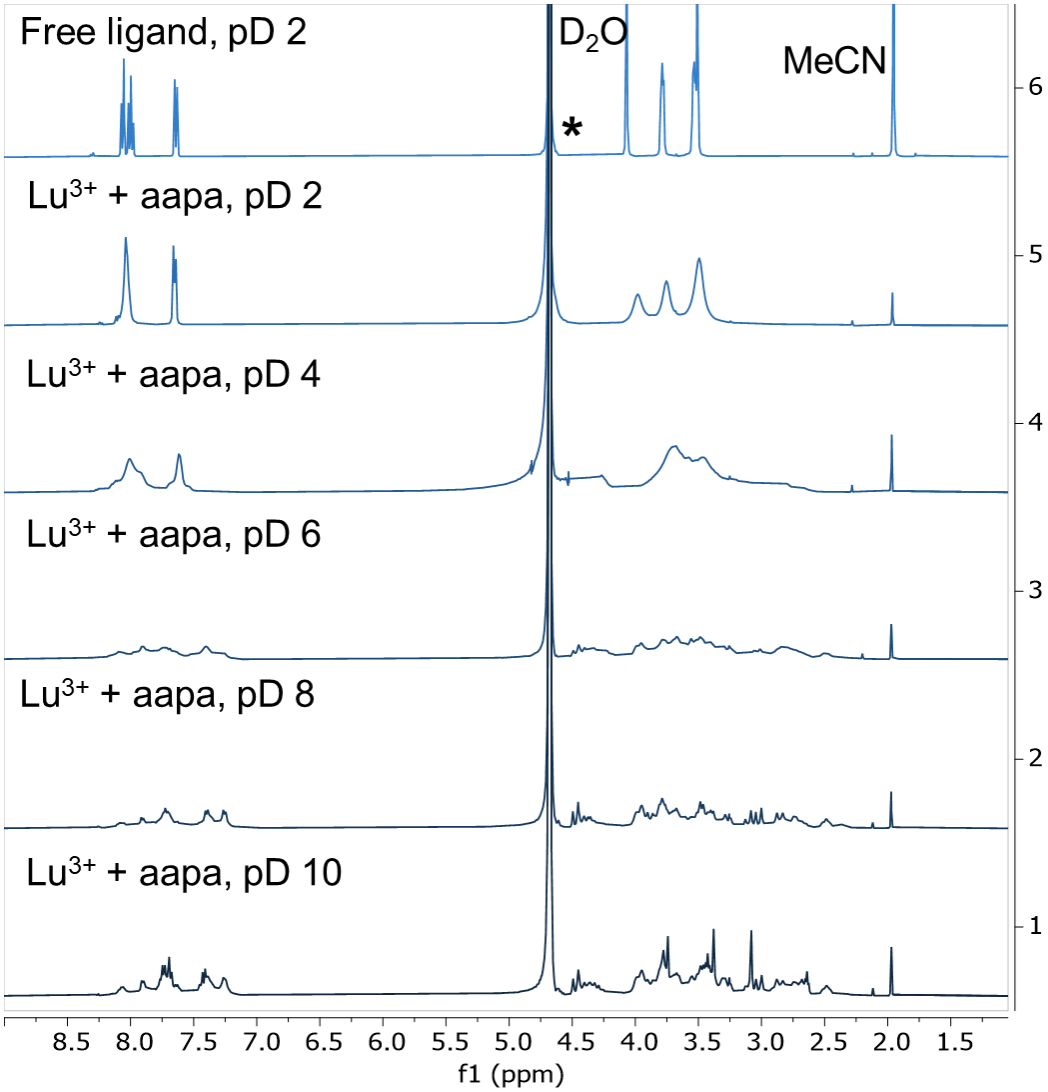

Figure S19. ^{1}H NMR spectra of free ligand at pD 2 and a 1:1 mixture of Lu^{3+} and aapa at different pD values. Acetonitrile was added as an internal reference.

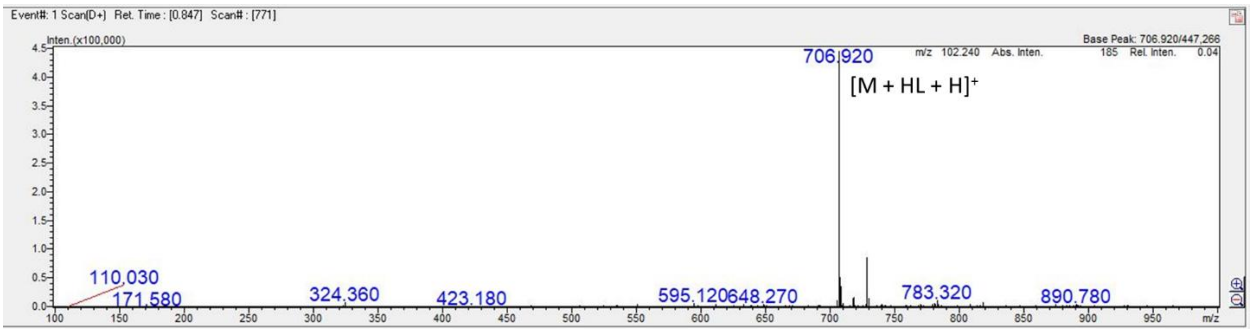

Figure S20. MS of 1:1 mixture of Lu^{3+} and aapa.

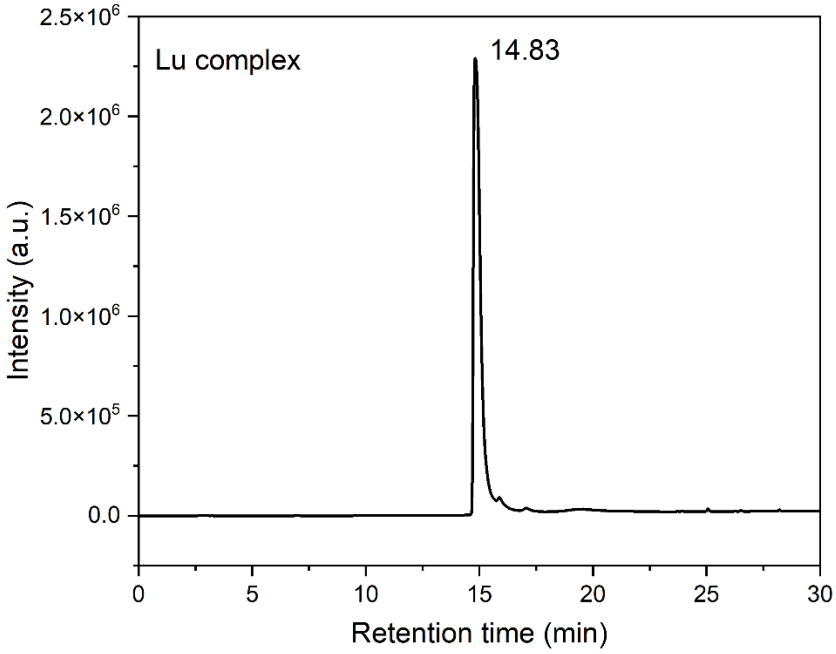

Figure S21. HPLC chromatogram of 1:1 mixture of Lu^{3+} and aapa (Method quick-MeOH, 270 nm detector).

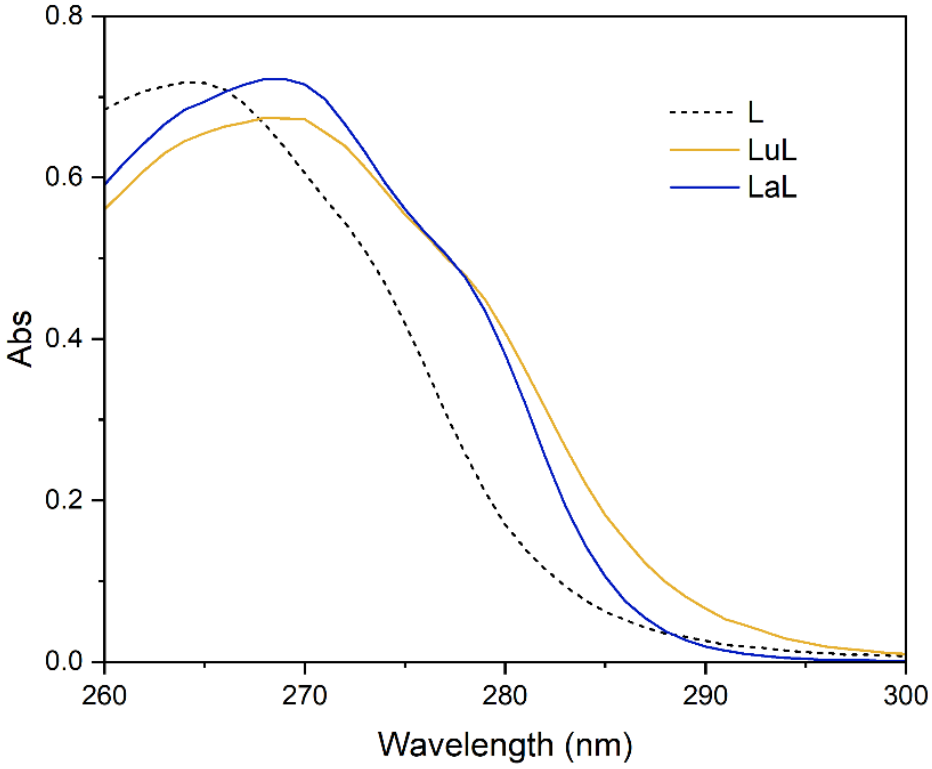

Figure S22. UV-Vis spectra of aapa, La–aapa and Lu–aapa (50 μM, pH 7.4, 100 mM MOPS).

Table S1. Synthesis cost of macropa

Product	Chemicals	Quantity of chemical used	Price ($)
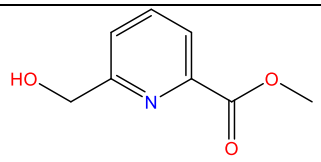	dimethyl pyridine-2,6-dicarboxylate	15 g	5.9
	$NaBH_4$	5.78 g	2.7
	MeOH	140 mL	3.2
	DCM	60 mL	1.7
	$NaHCO_3$	10 g	1.3
	$CHCl_3$	150 ml	7.6
	Na_2SO_4	20 g	2.4
	Yield: 10.5 g (82%)	Total cost: $25	
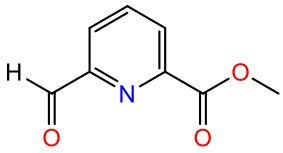	Chemicals	Chemical weight used	Price ($)
	arm-OH	5 g	11.9
	SeO_2	5 g	4.8
	1,4-dioxane	120 ml	9.15
	$CHCl_3$	150 ml	7.6
	Yield: 4.7 g (94%)	Total cost: $33.5	
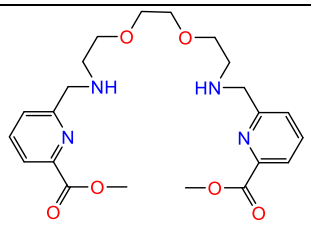	Chemicals	Chemical weight used	Price ($)
	2,2′-(Ethylenedioxy)bis(ethylamine)	2 ml	1.62
	CHO-arm	4.48 g	31.9
	CH_3OH	150 mL	3.4
	$NaBH_4$	600 mg	0.6
	$NaHCO_3$	8 g	0.8
	DCM	200 ml	4.2
	Na_2SO_4	20 g	0.56
	Yield: 5.2 g	Cost: $43.1	
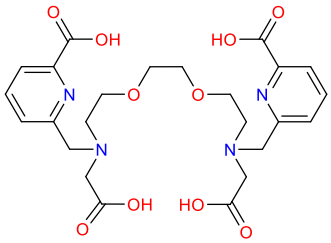	dimethyl 6,6'-(5,8-dioxa-2,11-diazadodecane-1,12-diyl)dipicolinate	5.2 g	43.1
	methyl 2-bromoacetate	5.13	4.6
	MeCN	100 mL	2.8
	NaCO3	5 g	0.5
	DCM	150 mL	3.18
	HCl	20 mL (6 M)	1
	Acetone	150 mL	1.2
	Yield: 4.9 g (aapa•$3H_2O$•5HCl)	Total cost: $56.1 g	

Table S2. Synthesis cost of macropa

Product	Chemicals	Chemical weight used	Price ($)
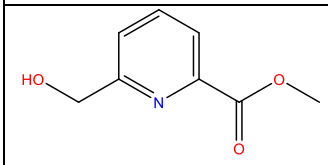	dimethyl pyridine-2,6-dicarboxylate	15 g	5.9
	$NaBH_4$	5.78 g	2.7
	MeOH	140 mL	3.2
	DCM	60 mL	1.7
	$NaHCO_3$	10 g	1.3
	$CHCl_3$	150 ml	15.8
	Na_2SO_4	20 g	2.4
	Yield: 10.5 g (82%)	Total cost: $24.8	
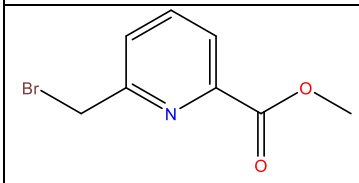	Chemicals	Chemical weight used	Price ($)
	arm-OH	5 g	15.6
	PBr_3	2.4 ml	2.3
	$CHCl_3$	300 ml	3.2
	K_2CO_3	10 g	1.4
	Diethyl ether	50 ml	4.8
	Yield: 6.50 g (94.6%)	Total cost: $27.33	
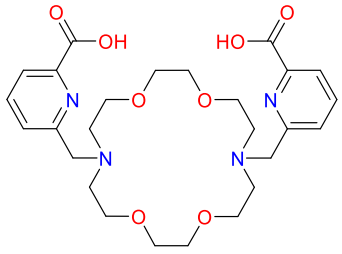	Chemicals	Chemical weight used	Price ($)
	K22	2 g	140
	Na_2CO_3	5 g	0.5
	Bromo-arm	3.5 g	14.7
	acetonitrile	50 mL	1.41
	DCM	150 mL	3.18
	HCl	20 mL (6 M)	1
	Acetone	150 mL	1.2
	Yield: 3.8 g (77%, macropa•$3H_2O$•3HCl)	Total cost: $162	

S2. X-ray crystallography

S2.1 Experimental details

X-ray quality crystals of [La(H_2aapa)][La(aapa)] were obtained via the following procedure. Aapa 3HCl 3H_2O (30 mg, 1 eq, 0.043 mmol) was dissolved in water (3 mL). To this solution, a solution of $LaCl_3 \cdot 7H_2O$ (17 mg, 1.3 eq, 0.047 mmol) in 0.5 mL water was added. The pH of this solution was adjusted to 4 using 0.1 M NaOH (300 µL), and the resulting mixture was stirred at room temperature for 1 h followed by lyophilization of this solution to give a white powder, which was redissolved in 1 mL MeOH. This complex solution in MeOH was filtered and crystals suitable for X-ray crystallography were obtained by slow evaporation of the filtrate (the vial was capped) at room temperature over a month.

Low-temperature X-ray diffraction data for the La–aapa complex was collected on a Bruker kappa apex 2 diffractometer coupled to a CCD detector and 2Kw Mo Kα radiation (λ = 0. 71073 Å) with TRIUMPH monochromator. The system is also equipped with Oxford 700 Plus Cryostream, which perform temperature-dependent measurement at 100 K. The diffraction images were processed and scaled using the Olex2-1.5 software.[2] The structure was solved through intrinsic phasing using SHELXT and refined against F^2 on all data by full-matrix least squares with SHELXL following established refinement strategies.[3–5] All non-hydrogen atoms were refined anisotropically. All hydrogen atoms bound to carbon were included in the model at geometrically calculated positions and refined using a riding model. Hydrogen atoms bound to oxygen were located in the difference Fourier synthesis and subsequently refined semi-freely with the help of distance restraints. The isotropic displacement parameters of all hydrogen atoms were fixed to 1.2 times the U_{eq} value of the atoms they are linked to (1.5 times for methyl groups). For this structure, there was pseudo-symmetry relating the two La^{3+} complexes, which both resided on crystallographic 2-fold rotation axes. This pseudo-symmetry led to large correlation matrices between several C atoms on the main residue. Consequently, their anisotropic displacement parameters were constrained to be identical. In addition, disordered electron density was apparent within the unit cell. This disorder could satisfactorily be refined as a partially occupied water and methanol molecules occupying the same region of space. The CheckCIF algorithm identified an A- and B-level alerts, related to close contacts between donor atoms in the crystal. In looking at these atoms, the close contacts can reasonably be explained by hydrogen bonding. Details of the data quality and a summary of the residual values of the refinements are listed in Tables S3–S4. Crystallographic data are available from the Cambridge Crystallographic Database Centre under accession code 2528345.

Table S3. Crystal data and structure refinement for [La(H_2aapa)][La(aapa)]

Empirical formula	$C_{48.91}H_{72.72}N_8O_{30}La_2$
Formula weight	1530.54
Temperature	100.04 K
Wavelength	0.71073 Å
Crystal system	Monoclinic
Space group	*P2/c*
Unit cell dimensions	a = 20.903(3) Å α= 90° b = 8.2203(10) Å β= 105.955(8)° c = 17.5505(19) Å γ = 90°
Volume	2899.5(6) $Å^3$
Z	2
Density (calculated)	1.753 Mg/m^3
Absorption coefficient	1.555 mm^{-1}
F(000)	15562.0
Crystal size	0.239 × 0.166 × 0.133 mm^3
Theta range for data collection	2.026 to 53.75°
Index ranges	–21< = h < = 26, –9< = k< =10, -22< = l< = 22
Reflections collected	12604
Independent reflections	6128 [R_{int} = 0.0471, R_{sigma} = 0.0745]
Completeness to theta = 25.242°	99.9 %
Absorption correction	Gaussian
Max. and min. transmission	1.000 and 0.446
Refinement method	Full-matrix least-squares on F^2
Data / restraints / parameters	6128 / 35 / 428
Goodness-of-fit on F^2	1.018
R1/wR2 [I>2sigma(I)]	R1 = 0.0408, wR2 = 0.0721
R1/wR2 (all data)	R1 = 0.0624, wR2 = 0.0793
Largest diff. peak and hole	0.72 and -0.63 e. $Å^{-3}$

$R1 = \Sigma||F_o| - |F_c||/|F_o|$; $wR2 = \{\Sigma[w(F_o^2 - F_c^2)2]/\Sigma[w(F_o^2)^2]\}^{1/2}$

$GoF = \{\Sigma[w(F_o^2 - F_c^2)2]/(n - p)\}^{1/2}$, where n is the number of data and *p* is the number of refined parameters.

Table S4. Interatomic distances [Å] for the structure of the [La(aapa)][La(H_2aapa)].

$[La(aapa)]^-$		$[La(H_2aapa)]^+$	
La(2)–N(1)	2.736(3)	La(1)–N(01)	2.739(3)
La(2)–N(2)	2.780(3)	La(1)–N(02)	2.798(3)
La(2)–O(2)	2.619(2)	La(1)–O(01)	2.620(3)
La(2)–O(5)	2.618(3)	La(1)–O(05)	2.535(3)
La(2)–O(4)	2.453(3)	La(1)–O(04)	2.493(3)
La(2)–N(1)	2.736(7)	La(1)–N(01)	2.739(3)
La(2)–N(2)	2.736(7)	La(1)–N(02)	2.798(3)
La(2)–O(2)	2.780(3)	La(1)–O(01)	2.620(3)
La(2)–O(5)	2.618(3)	La(1)–O(05)	2.535(3)
La(2)–O(4)	2.453(3)	La(1)–O(04)	2.493(3)

The atoms are labelled in Figure 1 of the main text.

S3. Solution thermodynamic

S3.1. Potentiometric titration

The protonation constants of H_4aapa were determined potentiometrically on a Metrohm Titrando 888 titrator equipped with a Ross Orion combination electrode (8103BN, ThermoFisher Scientific) and a Metrohm 806 exchange unit with an automatic burette (10 mL). This titration system was controlled by Tiamo (ver. 2.5) software. The titration vessel was fitted into a removable glass cell ($\approx$ 70 mL) and thermostated at 25.0 °C (pK_w = 13.78)[6] using a Thermomix 1442D circulating water bath. CO_2 was purged from the vessel prior to and during the titrations under a positive pressure of argon, which was passed through an aqueous 30 wt% KOH solution. Carbonate-free KOH (0.1 M, Honeywell) was standardized by potentiometric titration against potassium hydrogen phthalate. HCl (0.1 M, J.T. Baker) was standardized by potentiometric titration against Tris (base form). Titration solutions were maintained at a constant ionic strength of 0.1 M with KCl (BioUltra, $\geqslant$ 99.5%, Sigma-Aldrich) and were equilibrated for 15 minutes prior to the addition of titrant. The electrode was calibrated before each titration by titrating a solution of standardized HCl with standardized KOH, and the data were analyzed using the program Glee[7] to obtain the standard electrode potential and slope factor.

Ligand stock solutions ($\approx$ 20 mM for aapa) were made by dissolving the solid ligand in H_2O, and their exact concentrations were determined based on the end points of the potentiometric titration curves obtained during the protonation constant measurements. The concentrations determined from titration curves matched the concentrations calculated from the ligand masses using molecular weights obtained from elemental analysis results. Cu^{2+} and Fe^{2+} standard solutions were used for titration. Ln^{3+} stock solutions were made by dissolving the corresponding $LnCl_3$ hydrate salts (>99.9% purity) in standardized HCl (0.1 M). Their exact concentrations were determined by complexometric titrations with 1 mM standardized Na_2H_2EDTA solution (diluted from 50 mM, Alfa Aesar). The complexometric titrations were conducted at pH 5.5 maintained by a NH_4OAc buffer (100 mM), and the end point was indicated by xylenol orange.[8]

Protonation constant measurements were carried out by titrating an aqueous solution ($\approx$20 mL) of free ligand ($\approx$1 mM) and HCl ($\approx$ 5 mM) with standardized KOH (0.1 M). Stability constant measurements were carried out by titrating an aqueous solution ($\approx$15 mL) of ligand ($\approx$1 mM), metals ($\approx$0.95 mM), and HCl ($\approx$5 mM) with standardized KOH (0.1 M). The ionic strength of the solution was maintained at 0.1 M using 1 M KCl. The titration method employed a 0.1 mV/min drift limit. Up to 3 mins for protonation constant and 5 mins for stability constant of wait time between two addition KOH aliquots was given to reach equilibrium and record the pH of solution. Hyperquad2013 software was used for the analysis of the titration data within the pH range of 2.5–11.3.[9] Both protonation constants and stability constants were calculated from the average of three independent titrations using three independently prepared stock solutions from three independent synthetic preparations of ligands.

The protonation constants (K_a) and stability constants (K_{LnL}), obtained from the Hyperquad data analysis, can be expressed as Equations. S1 and S2, where the concentration terms represent the equilibrium concentrations of these species.

$$K_a = [H_iL]/[H^+]\,[H_{i-1}L] \qquad \text{(Eq. S1)}$$

$$K_{LnL} = [LnL]/[Ln^{3+}]\,[L] \qquad \text{(Eq. S2)}$$

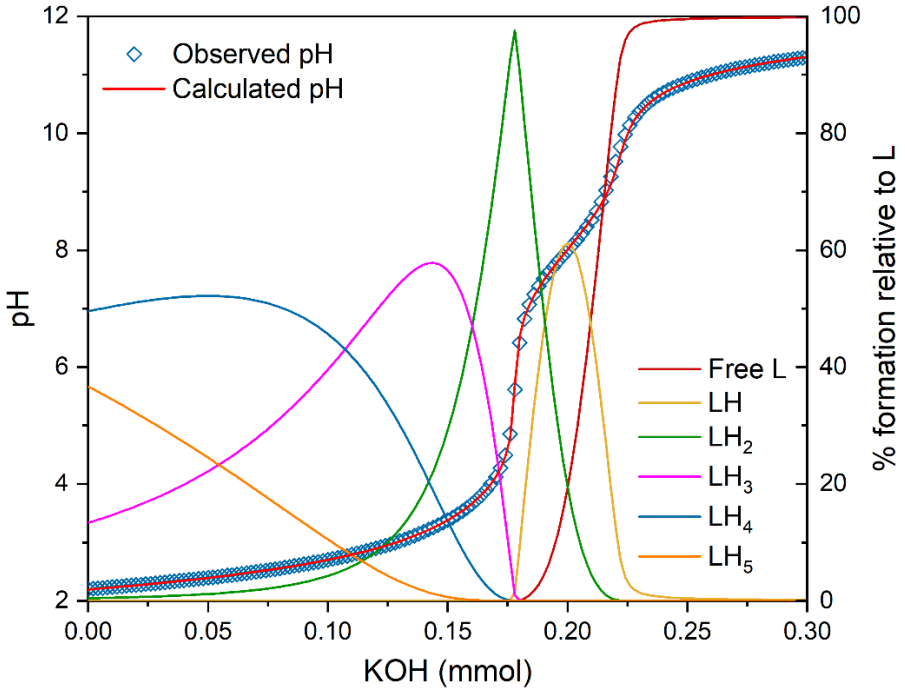

Figure S23. Representative protonation constant determination of H_4aapa by potentiometric titrations. C_{aapa} = 1 × 10^{-3} M. Initial volume V = 20 mL. Data fitting and speciation distribution over the titration pH range are shown. Sigma value of this refinement =0.513.

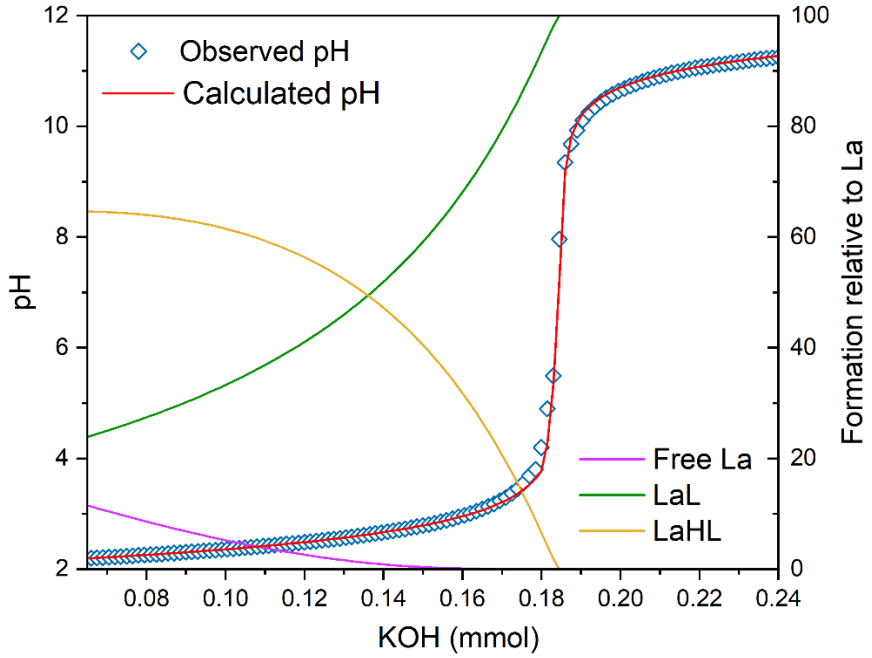

Figure S24. Representative stability constant determination of La–aapa system by potentiometric titrations. C_{La} = 9.5 × 10^{-4} M, C_{aapa} = 1 × 10^{-3} M. Initial volume V = 15 mL. Data fitting and speciation distribution over the titration pH range are shown. The sigma value of this refinement = 2.930.

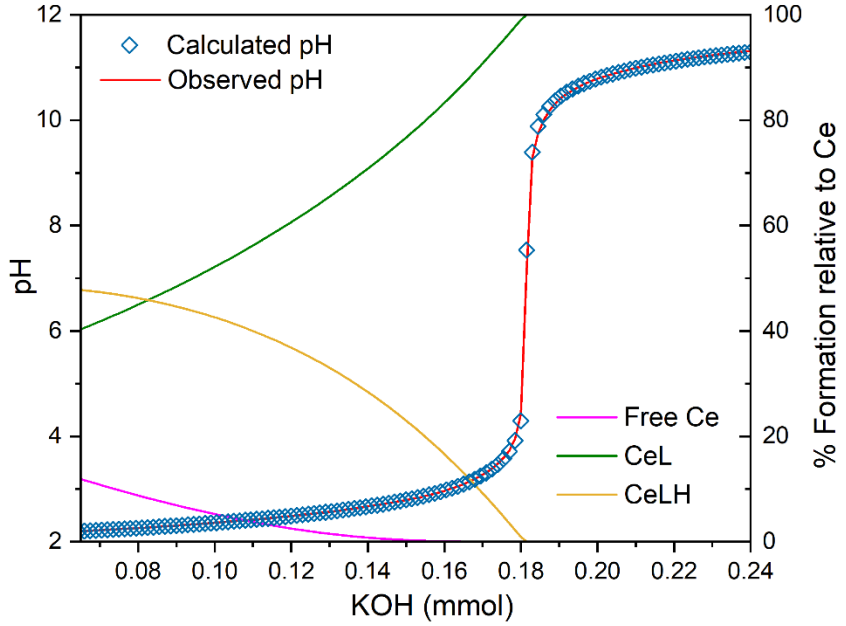

Figure S25. Representative stability constant determination of Ce–aapa system by potentiometric titrations. C_{Ce} = 9.5 × 10^{-4} M, C_{aapa} = 1 × 10^{-3} M. Initial volume V = 15 mL. Data fitting and speciation distribution over the titration pH range are shown. The sigma value of this refinement = 1.456.

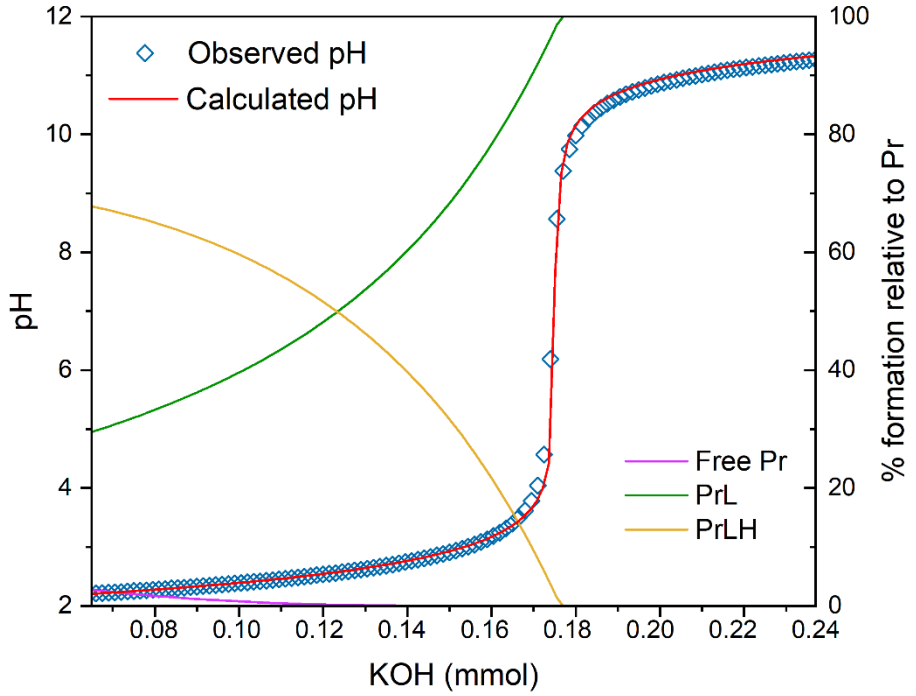

Figure S26. Representative stability constant determination of Pr–aapa system by potentiometric titrations. C_{Pr} = 9.5 × 10^{-4} M, C_{aapa} = 1 × 10^{-3} M. Initial volume V = 15 mL. Data fitting and speciation distribution over the titration pH range are shown. The sigma value of this refinement = 1.655.

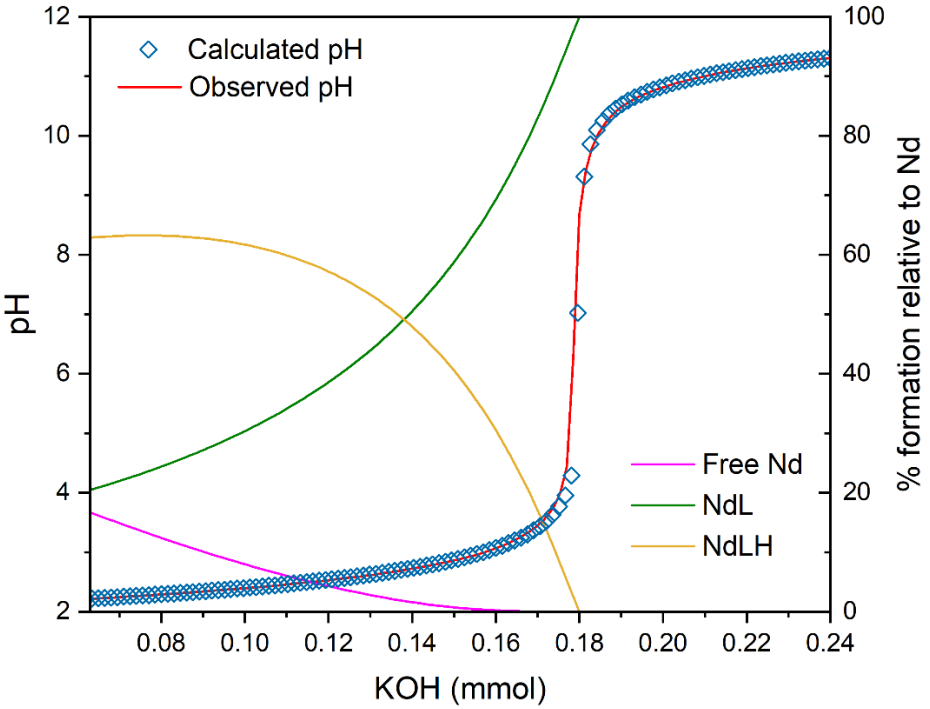

Figure S27. Representative stability constant determination of Nd–aapa system by potentiometric titrations. C_{Nd} = 9.5 × 10^{-4} M, C_{aapa} = 1 × 10^{-3} M. Initial volume V = 15 mL. Data fitting and speciation distribution over the titration pH range are shown. The sigma value of this refinement = 1.611.

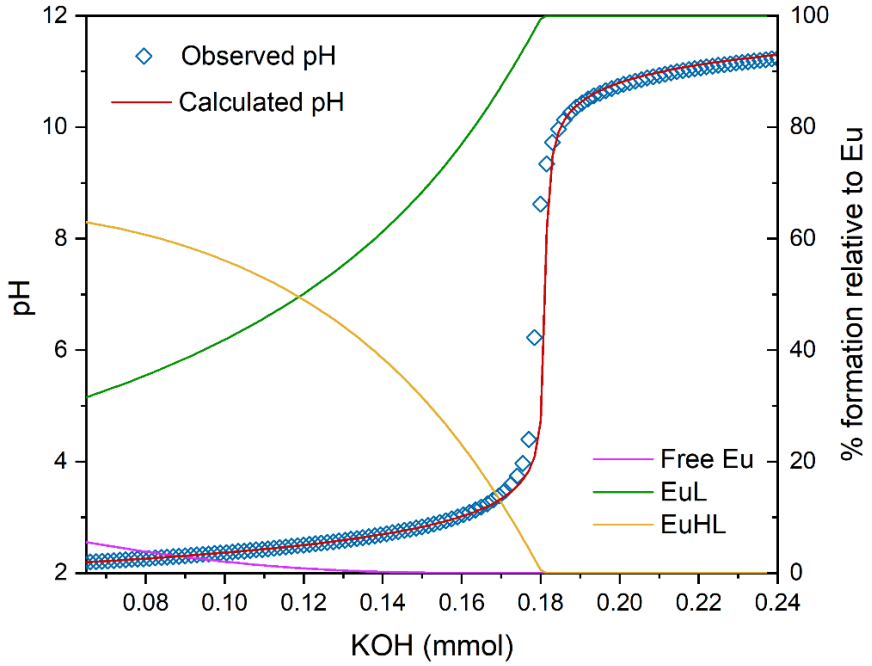

Figure S28. Representative stability constant determination of Eu–aapa system by potentiometric titrations. C_{Eu} = 9.5 × 10^{-4} M, C_{aapa} = 1 × 10^{-3} M. Initial volume V = 15 mL. Data fitting and speciation distribution over the titration pH range are shown. The sigma value of this refinement = 3.697.

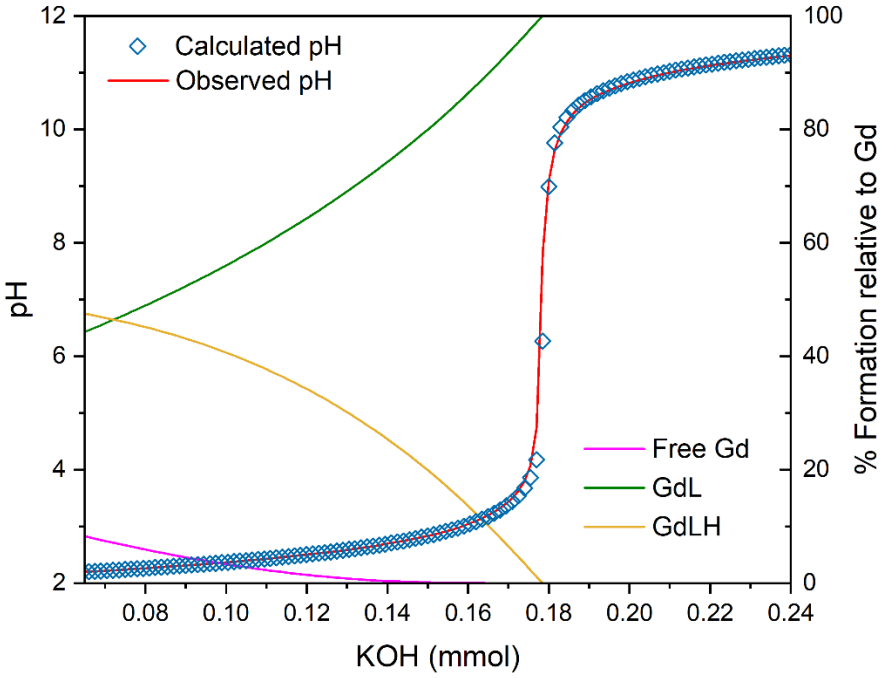

Figure S29. Representative stability constant determination of Gd–aapa system by potentiometric titrations. C_{Gd} = 9.5 × 10^{-4} M, C_{aapa} = 1 × 10^{-3} M. Initial volume V = 15 mL. Data fitting and speciation distribution over the titration pH range are shown. The sigma value of this refinement = 1.019.

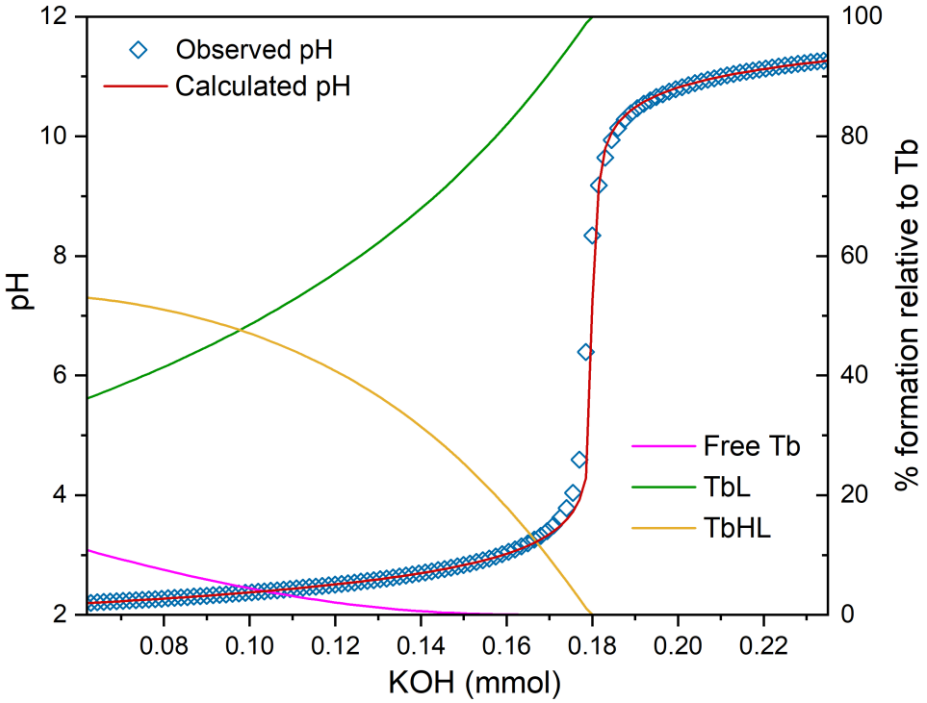

Figure S30. Representative stability constant determination of Tb–aapa system by potentiometric titrations. C_{Tb} = 9.5 × 10^{-4} M, C_{aapa} = 1 × 10^{-3} M. Initial volume V = 15 mL. Data fitting and speciation distribution over the titration pH range are shown. The sigma value of this refinement = 1.210.

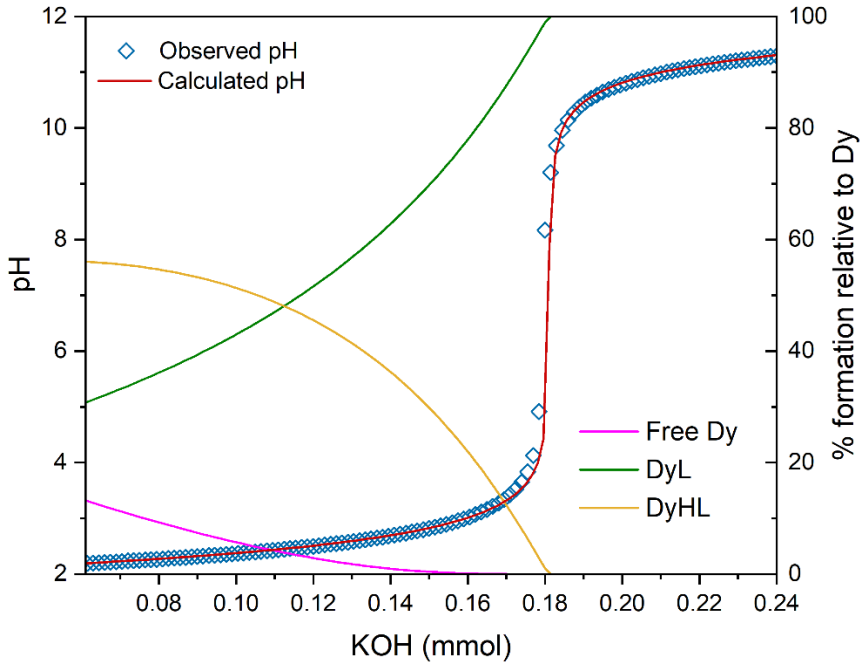

Figure S31. Representative stability constant determination of Dy–aapa system by potentiometric titrations. C_{Dy} = 9.5 × 10^{-4} M, C_{aapa} = 1 × 10^{-3} M. Initial volume V = 15 mL. Data fitting and speciation distribution over the titration pH range are shown. The sigma value of this refinement = 0.508.

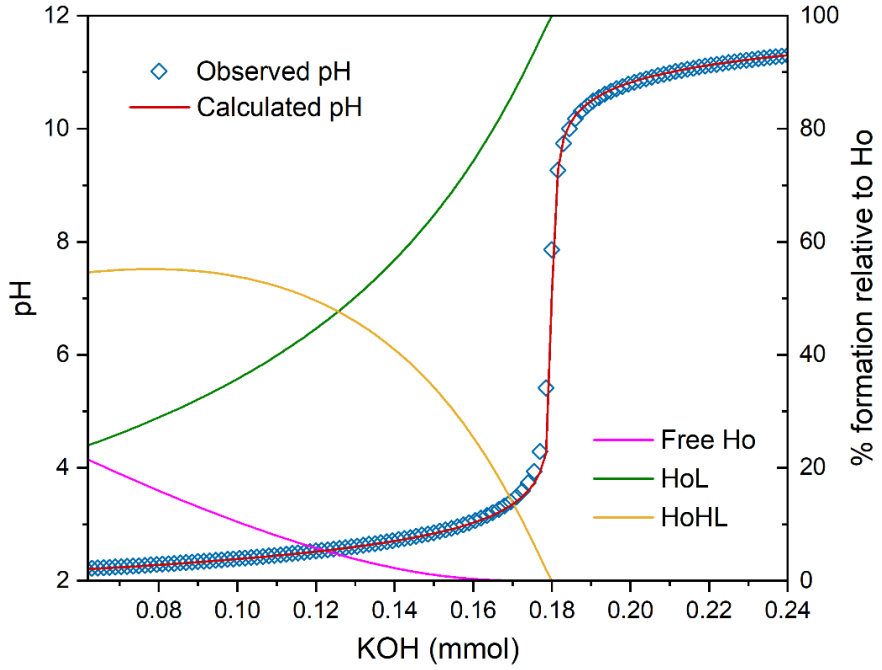

Figure S32. Representative stability constant determination of Ho–aapa system by potentiometric titrations. C_{Ho} = 9.5 × 10^{-4} M, C_{aapa} = 1 × 10^{-3} M. Initial volume V = 15 mL. Data fitting and speciation distribution over the titration pH range are shown. The sigma value of this refinement = 0.904.

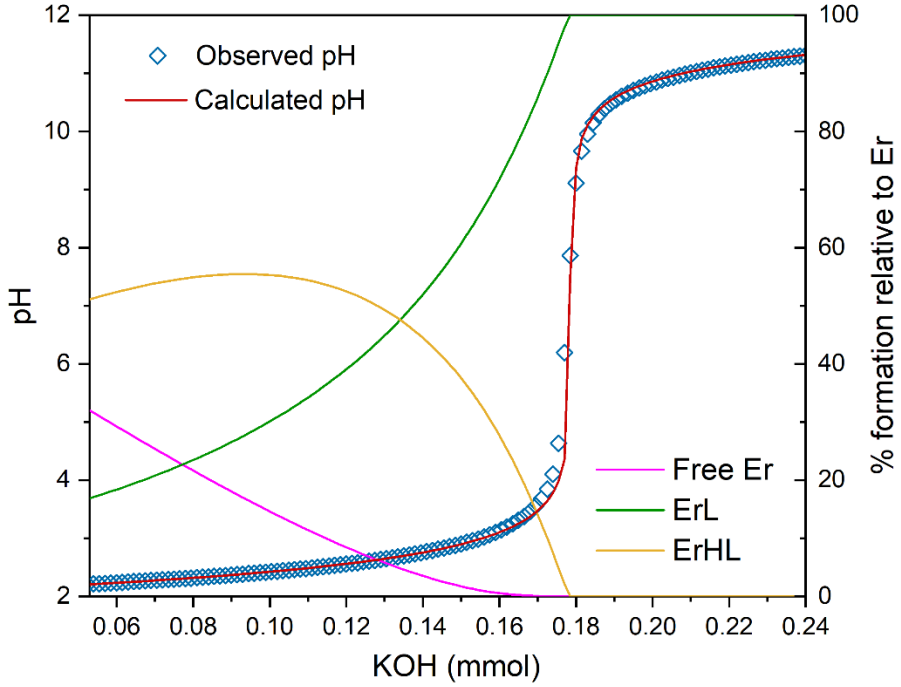

Figure S33. Representative stability constant determination of Er–aapa system by potentiometric titrations. C_{Er} = 9.5 × 10^{-4} M, C_{aapa} = 1 × 10^{-3} M. Initial volume V = 15 mL. Data fitting and speciation distribution over the titration pH range are shown. The sigma value of this refinement = 0.944.

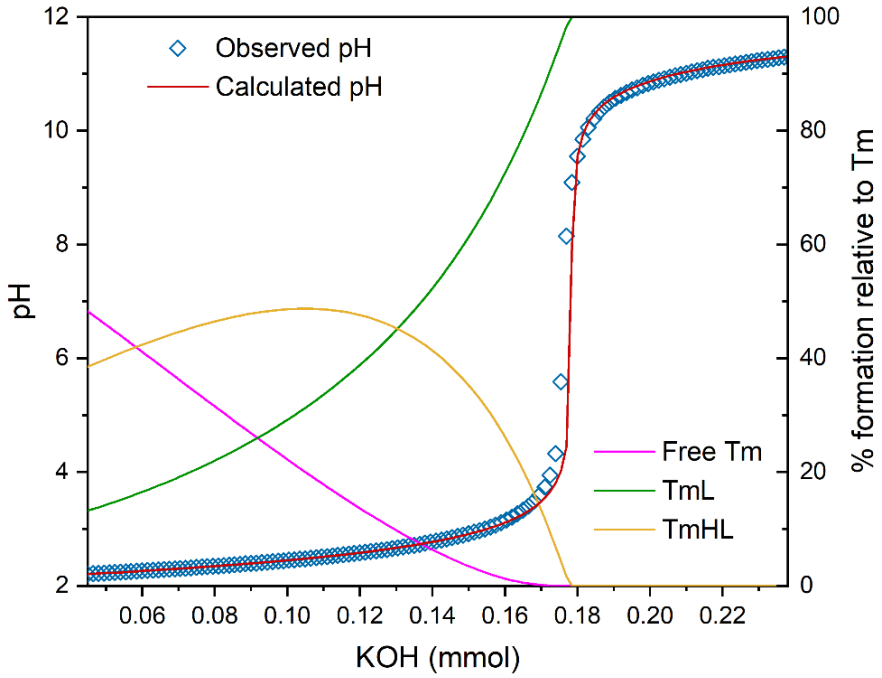

Figure S34. Representative stability constant determination of Tm–aapa system by potentiometric titrations. C_{Tm} = 9.5 × 10^{-4} M, C_{aapa} = 1 × 10^{-3} M. Initial volume V = 15 mL. Data fitting and speciation distribution over the titration pH range are shown. The sigma value of this refinement = 0.925.

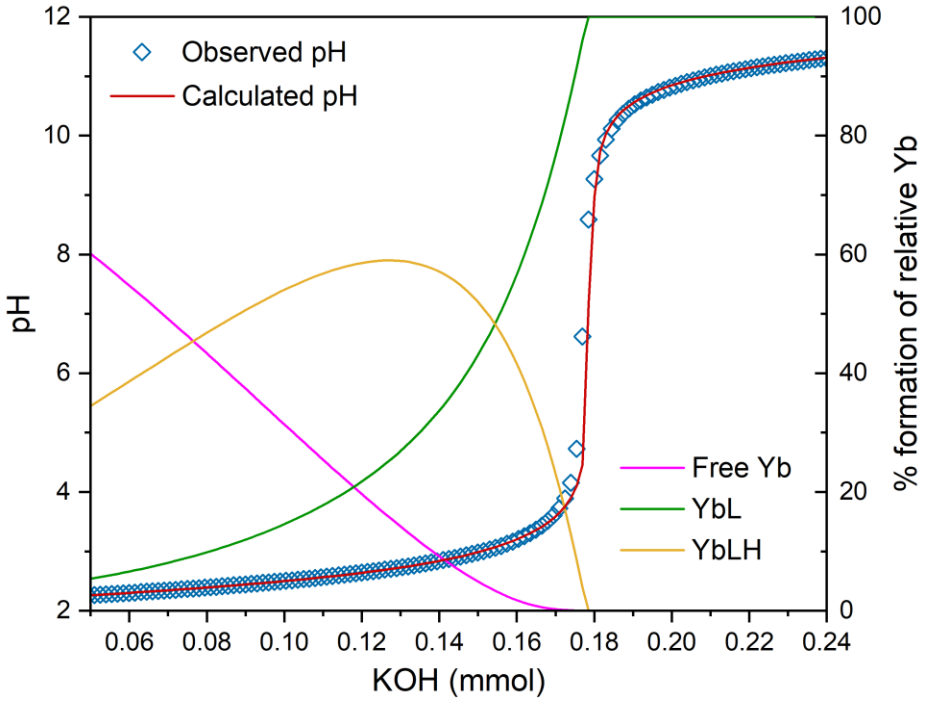

Figure S35. Representative stability constant determination of Yb–aapa system by potentiometric titrations. C_{Yb} = 9.5 × 10^{-4} M, C_{aapa} = 1 × 10^{-3} M. Initial volume V = 15 mL. Data fitting and speciation distribution over the titration pH range are shown. The sigma value of this refinement = 0.703.

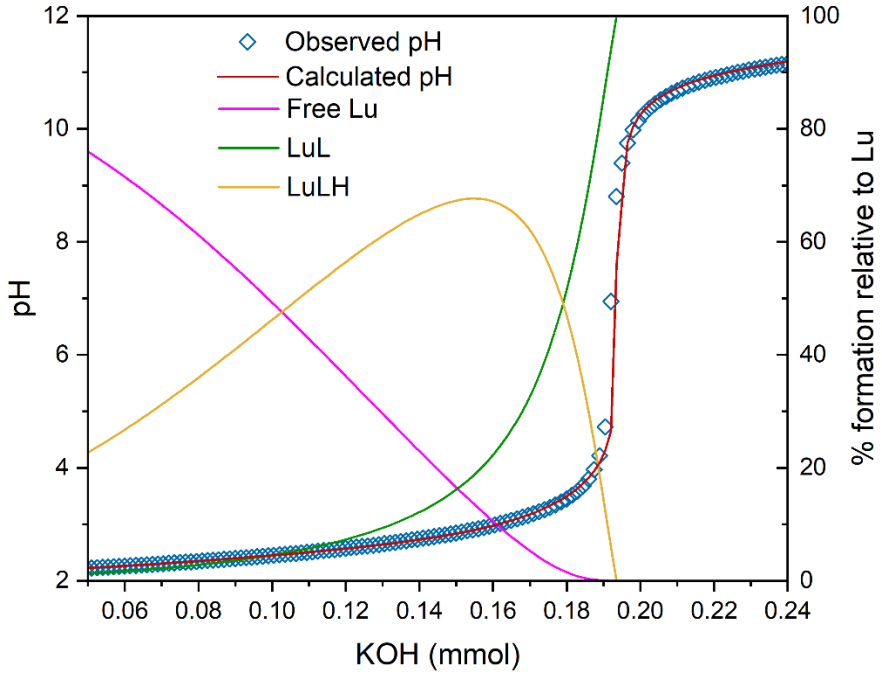

Figure S36. Representative stability constant determination of Lu–aapa system by potentiometric titrations. C_{Lu} = 9.5 × 10^{-4} M, C_{aapa} = 1 × 10^{-3} M. Initial volume V = 15 mL. Data fitting and speciation distribution over the titration pH range are shown. The sigma value of this refinement = 3.057.

S3.2. UV-vis titration

UV−vis spectra were recorded on a Shimadzu UV-1900 UV−Vis spectrometer with a 1 cm quartz cuvette. A series of solutions (15 samples) containing the ligand and La^{3+}, Ce^{3+}, Pr^{3+}, and Nd^{3+} in a 1:1 M:L ratio were prepared. The pH of each sample was adjusted with standardized 0.1 M HCl to span the range $1.28 \leq pH \leq 2.22$. The pH cannot be accurately measured using the glass electrode when $pH \leq 2.4$ and hence the pH was calculated directly from the concentration of HCl used in each sample. The ionic strength was adjusted to 0.1 M with KCl. All samples were allowed to equilibrate at 25 °C for at least 12 h. The pH-dependent spectroscopic data were analyzed using HypSpec 2014.[10] The absorption bands from 230–310 nm were used for analysis. Data are reported as mean ± SD of three independent titrations using stock solutions prepared from at least two independent preparations of ligand.

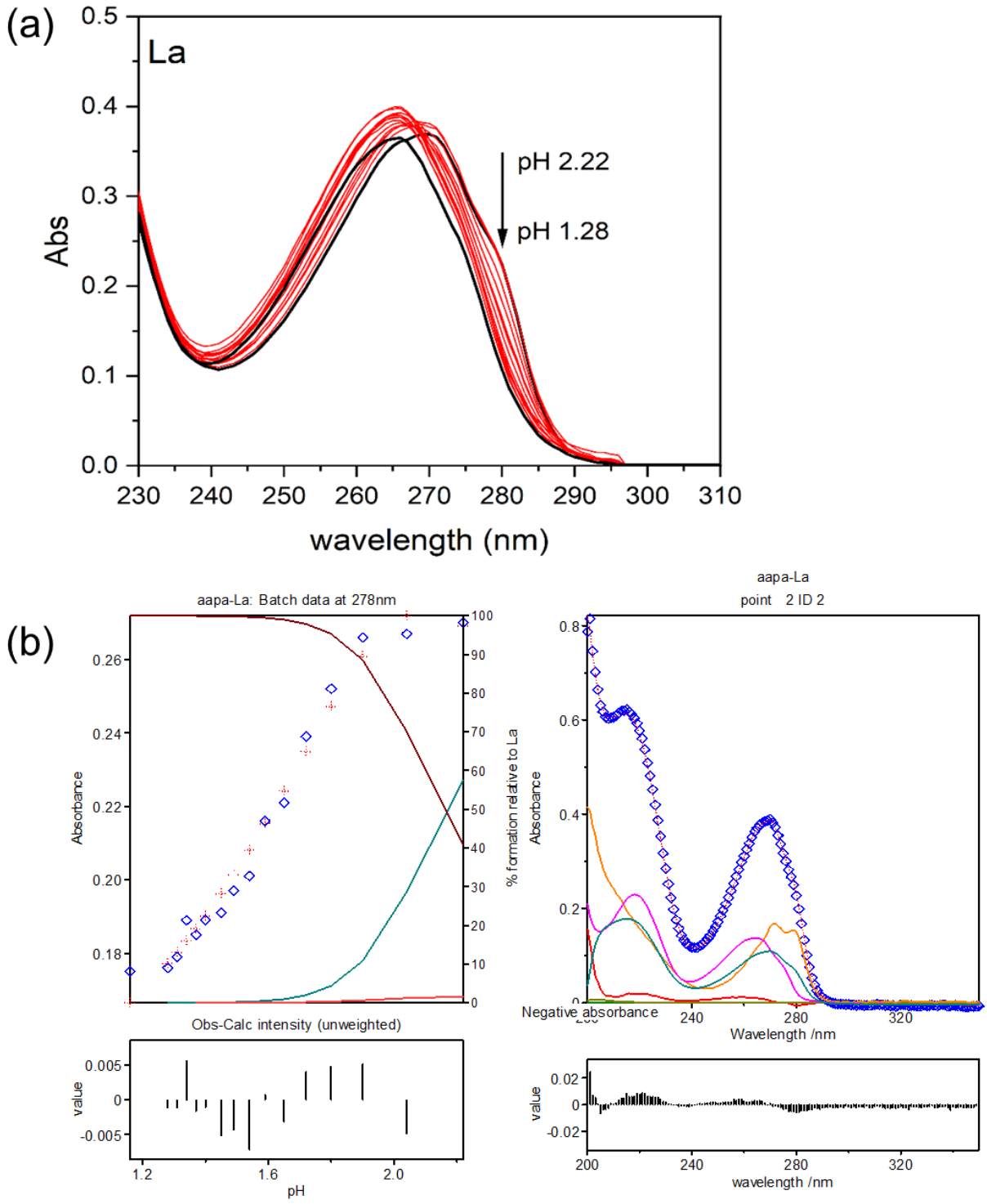

Figure S37. Representative UV–Vis spectrophotometric titration of La^{3+}–aapa system. C_{La} = c_{aapa} = 5 × 10^{-5} M. (a) UV–Vis spectral change over the titration pH range; (b) Data fitting at 278 nm and speciation distribution over the titration pH range.

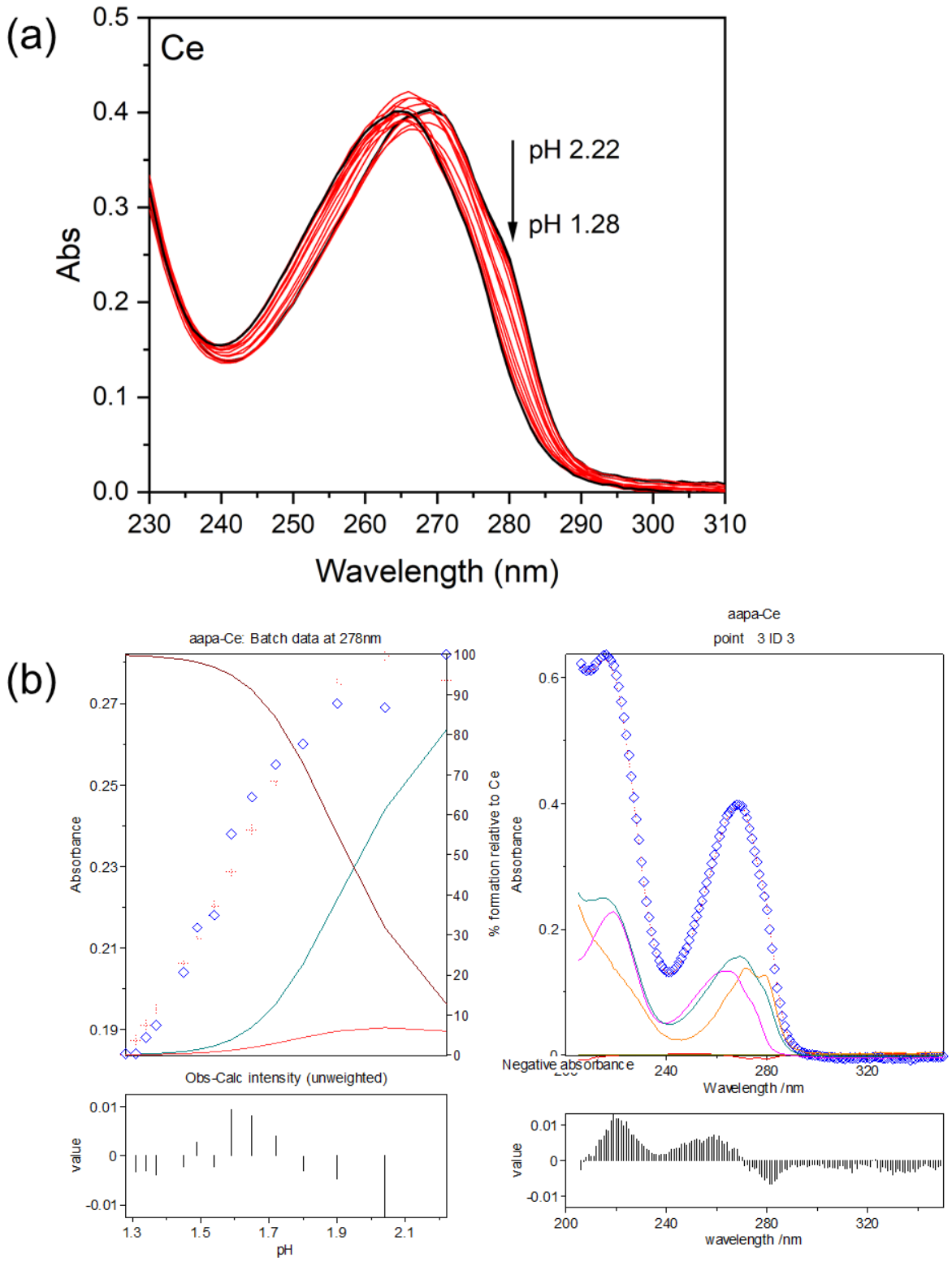

Figure S38. Representative UV–Vis spectrophotometric titration of Ce^{3+}–aapa system. $c_{Ce} = c_{aapa} = 5 \times 10^{-5}$ M. (a) UV–Vis spectral change over the titration pH range; (b) Data fitting at 278 nm and speciation distribution over the titration pH range.

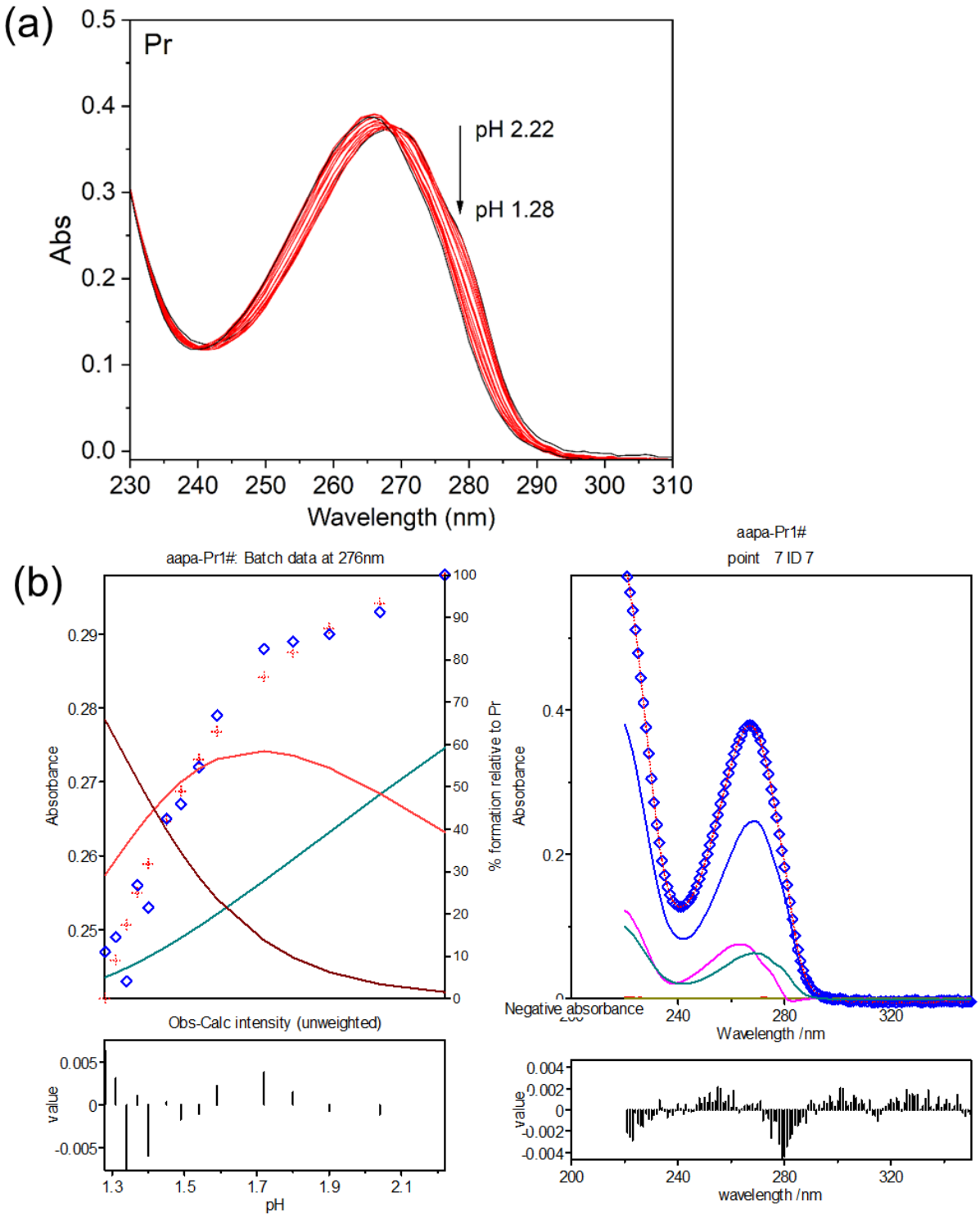

Figure S39. Representative UV–Vis spectrophotometric titration of Pr^{3+}–aapa system. C_{Pr} = c_{aapa} = 5 × 10^{-5} M. (a) UV–Vis spectral change over the titration pH range; (b) Data fitting at 278 nm and speciation distribution over the titration pH range.

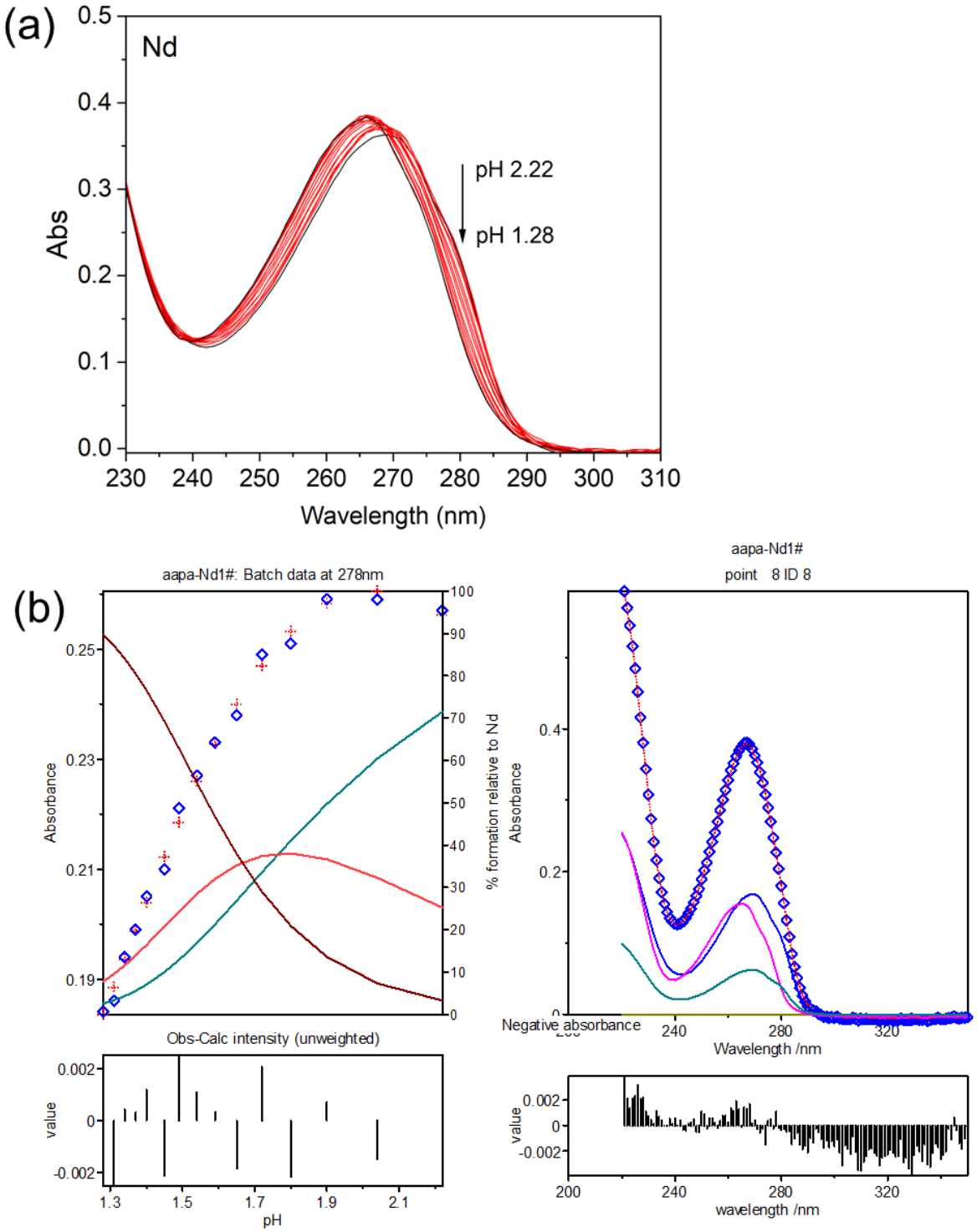

Figure S40. Representative UV–Vis spectrophotometric titration of Nd^{3+}–aapa system. $c_{Nd} = c_{aapa} = 5 \times 10^{-5}$ M. (a) UV–Vis spectral change over the titration pH range; (b) Data fitting at 278 nm and speciation distribution over the titration pH range.

Table S5. Stability constant of aapa with Cu^{2+} and Fe^{3+}.[a]

M	*p*M[b]	Species	log *K*
Cu^{2+}	6.3	Cu_2L	8.87(7)
		Cu_2LH	7.94(4)
		Cu_2LH_{-1}	-0.55(7)
Fe^{3+}	12.75	FeL	11.75
		FeLH	4.77
		$FeLH_2$	4.48
		$FeLH_{-1}$	3.54
		$FeLH_{-2}$	-3.93

[a]0.1 M KCl, results obtained from potentiometric titration (pH 2.2–11.3), this work.

[b] *p*M = –log $[M]_{free}$. Calculated for 10 μM total ligand and 1 μM total metal at pH 7.4 and 25 °C.

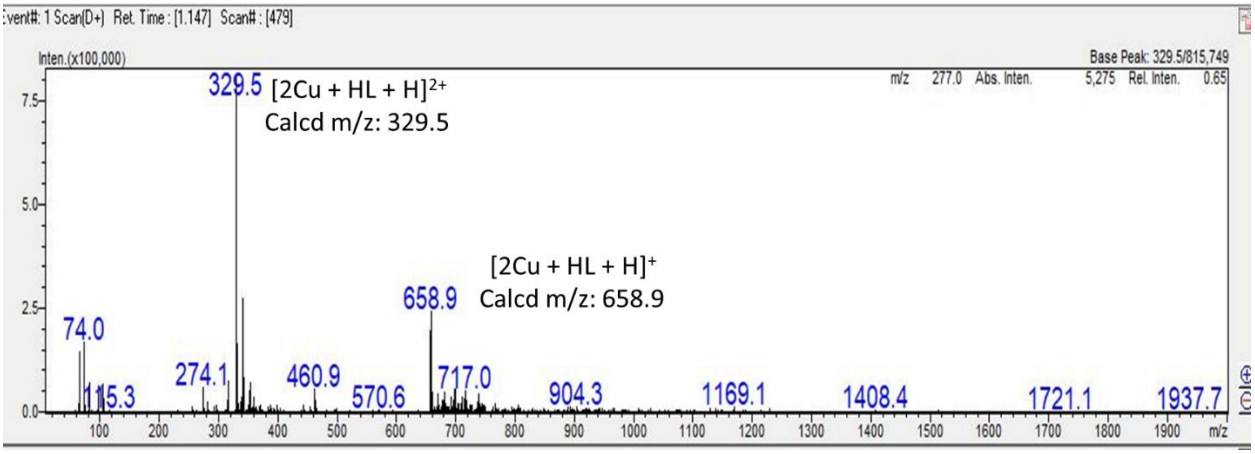

Figure S41. MS of 2:1 mixture of Cu^{2+} and aapa.

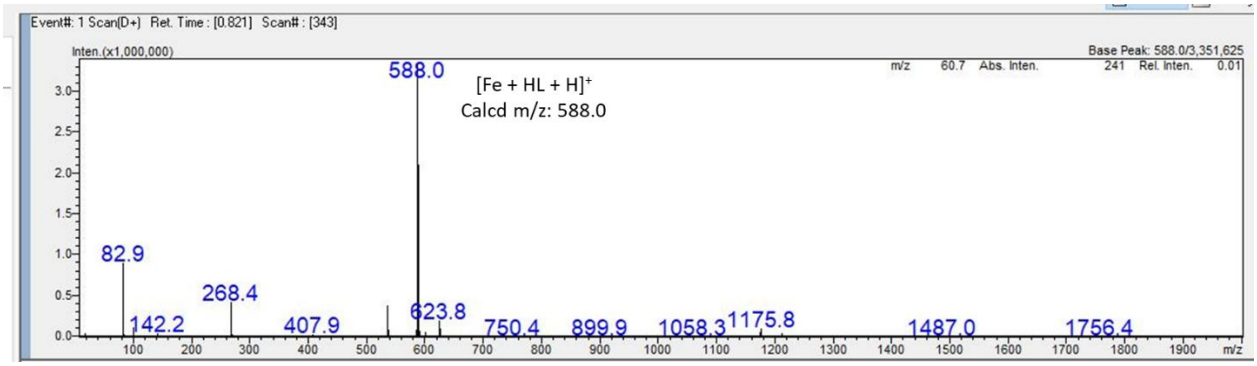

Figure S42. MS of 1:1 mixture of Fe^{3+} and aapa.

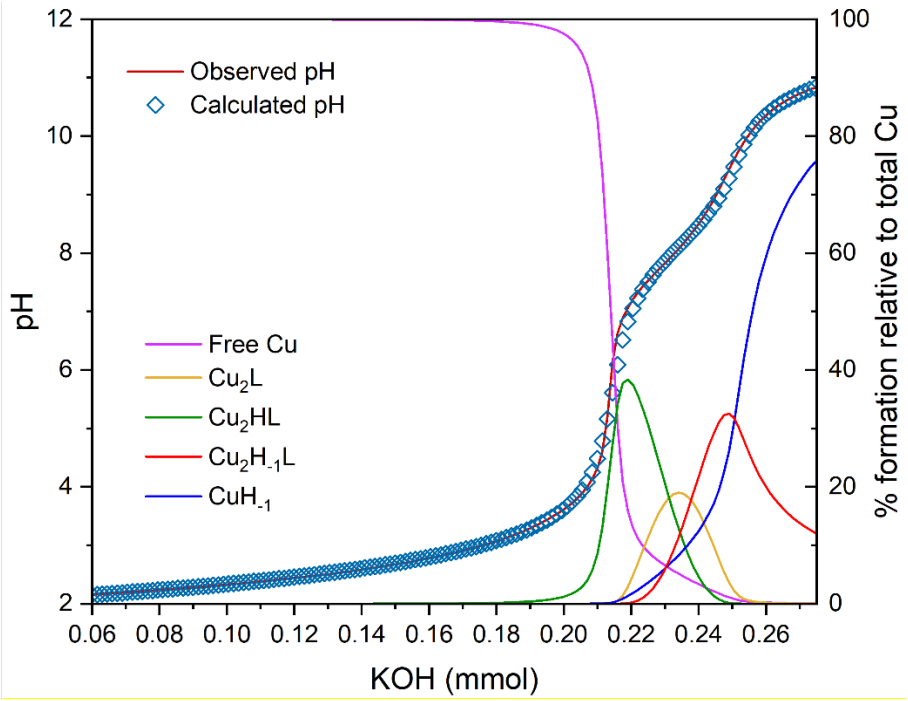

Figure S43. Representative stability constant determination of Cu–aapa system by potentiometric titrations. C_{Cu} = 1× 10^{-3} M, C_{aapa} = 1 × 10^{-3} M. Initial volume V = 15 mL. Data fitting and speciation distribution over the titration pH range are shown. The sigma value of this refinement = 2.195.

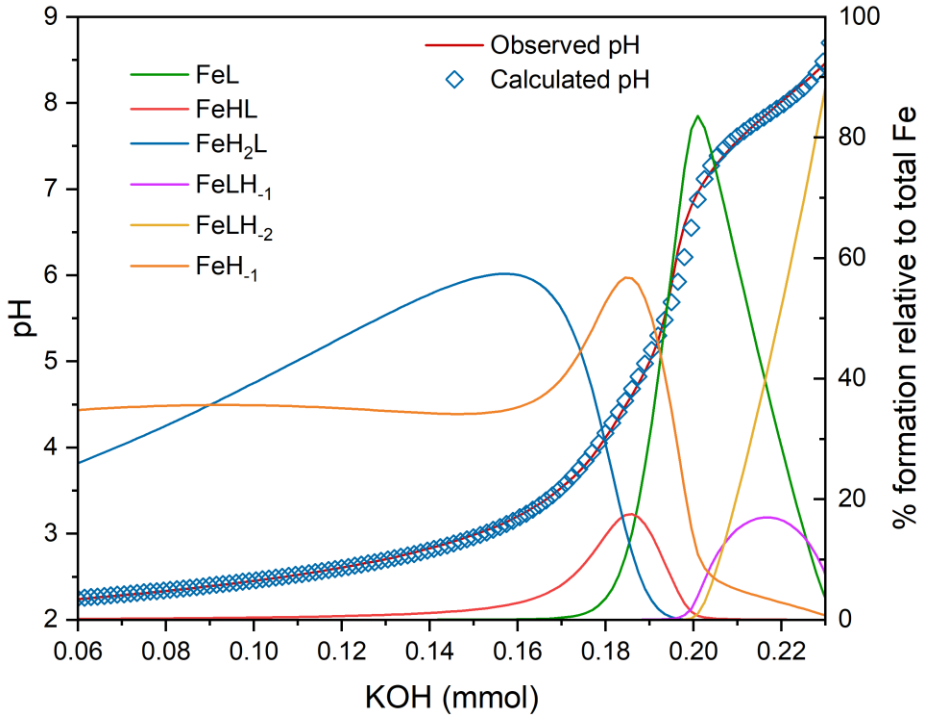

Figure S44. Representative stability constant determination of Fe–aapa system by potentiometric titrations. C_{Fe} = 1× 10^{-3} M, C_{aapa} = 1 × 10^{-3} M. Initial volume V = 15 mL. Data fitting and speciation distribution over the titration pH range are shown. The sigma value of this refinement = 3.036.

S4. Selective dissolution of REE oxalates and REE leaching from end-of-life materials.

4.1 Experimental details

4.1.1 Solution preparation

Aapa (20.16 mM) and macropa (20.70 mM) stock solutions were prepared in milli-Q water. The concentration of the two ligands were accurately determined by endpoint analysis of a pH potentiometric titration using a standardized KOH solution. DTPA stock solution (20 mM) were prepared in milli-Q water. The stock solution of ACS grade $(NH_4)_2C_2O_4$ (100 mM) was prepared in milli-Q water. The buffer stock solution (500 mM) was also prepared by dissolving ACS grade ammonium acetate (Fisher Scientific) in milli-Q water, and the pH was adjusted to 4, 4.5, and 5 by NaOH (5 M) and HCl (6 M). The electrode used to measure pH (Mettler Toledo FE20) was filled with 3 M NaCl and calibrated daily. The stock solutions of REEs were made by dissolving the $LnCl_3$ hydrate salts (99.9% purity or higher) in milli-Q water to a concentration of 100 mM. The $LnCl_3$ hydrate used in this study includes $LaCl_3•7H_2O$, $CeCl_3•6H_2O$, $PrCl_3•6H_2O$, $NdCl_3•6H_2O$, $GdCl_3•6H_2O$, $TbCl_3•6H_2O$, $DyCl_3•6H_2O$, $YbCl_3•6H_2O$, and $LuCl_3•6H_2O$.

4.1.2 Single REE Oxalates dissolution

All dissolution experiments were carried out at 22 ± 1 °C. The $LnCl_3$ stock solutions (10 µL) were combined with 40 µL of ammonium acetate buffer (pH 4, 4.5 and 5) and 30 µL $(NH_4)_2C_2O_4$ in a 96-well culture plate, and the solution was diluted to a total volume of 150 µL with milli-Q water. After a 30-min orbital shaking at 200 RPM to form the $REE_2(C_2O_4)_3$ precipitation, these suspensions were contacted with 50 µL of the 20 mM solution of aapa solution, affording a final REE concentration of 5 mM and allowed to mix for 1.5 h. The solids in resulting mixtures were removed by filtration with 220 nm nylon syringe filter. The filtrate was analyzed by ICP-OES after subjecting them to a 100-fold dilution with 2% nitric acid (50 µL → 5000 µL), and dissolution efficiency (*E*%) calculated using Eq. S3 and summarized in Table S5–S6. The concentration of buffered $LnCl_3$ solutions without adding ligand and $REE_2(C_2O_4)_3$ was determined by ICP-OES and was very close to 5 mM, confirming that the dilution and buffering treatment didn't lead to the concentration change of those solutions. All dissolution experiments were repeated in triplicates.

4.1.3 Selective dissolution of binary REE mixture at molar ratio of 1:1.

All dissolution experiments were carried out at 22 ± 1 °C. A 5 µL quantity of each $LnCl_3$ stock solutions were combined with 40 µL of ammonium acetate buffer (pH 4) and 30 µL of $(NH_4)_2C_2O_4$ in a 96-well culture plate, and the solution was diluted to a total volume of 150 µL with Milli-Q water. After a 30 min orbital shaking at 200 RPM to form the $REE_2(C_2O_4)_3$ precipitation, these suspensions were contacted with 50 µL of the 20 mM solution of aapa solution, affording a final REE concentration of 5 mM (2.5 mM of each) and allowed to mix for another 1.5 h. The solids in resulting suspensions were removed

by filtration with 220 nm nylon syringe filter. The filtrate was analyzed by ICP-OES after subjecting them to a 100-fold dilution with 2% nitric acid (50 µL → 5000 µL). The separation factors were calculated using Eq. S4 and summarized in Table S6. The concentration of buffered $LnCl_3$ solutions without adding ligand and $REE_2(C_2O_4)_3$ was determined by ICP-OES and was very close to 2.5 mM, confirming that the dilution and buffering treatment didn't lead to the concentration variation those solutions. All dissolution experiments were repeated in triplicates.

Dissolution efficiency (*E*%) of $REE_2(C_2O_4)_3$ solid is calculated using Eq. S3.

$$E\% = [REE_{filtrate}]/[REE_{initial}] \times 100\%$$

Separation factor (*SF*) is calculated using Eq S4.

$$SF_{REE1/REE2} = \frac{[REE1]solution \times [REE2]solid}{[REE1]solid \times [REE2]solution}$$

In this equation, REE1 represent lighter REEs, and REE2 represent heavier REEs.

All data from our separations are calculated based on the ICP concentrations determined in the filtrate, rather than from the digested or redissolved solid products. This approach, which has been used by others,[11] avoid errors with manipulating the solid precipitate that result from incomplete drying of the samples and losses due to mass transfer. Thus, the direct solution ICP measurements employed give more precise date that is less prone to error.

4.2 REE leaching from end-of-life materials

A sample of hard drive disc ground and separated at a 30-mesh size (0.595 mm) was provided by Dr. Erik Spiller and Dr. Brandon Ott at Colorado School of Mines (Golden, CO) by way of Dr. David Reed at Idaho National Lab. A smelting slag produced by the recycling of precious metals from catalytic converters was provided by REEgen, Inc. The chelator solution including aapa, macropa, DTPA solution was prepared dissolving their solid in milli-Q water, and buffered with 100 mM MOPS (pH 7.4) solution.

4.2.1 REEs leaching from magnet waste

A 20 mg quantity of magnet waste powder and 1 mL chelator (20 mM, pH 7.4) solution were combined in a 5 mL centrifuge tube and allowed to leach metals using an end-over-end rotation at 40 RPM for 24 h prior to remove undissolved solid by filtration. The resulting leachate composition was determined by ICP-OES after subjecting them to a 100-fold dilution with 2% nitric acid (50 µL → 5000 µL). All separation experiments were repeated in duplicate.

4.2.2 REEs leaching from autocat slag

A 50 mg quantity of autocat slag and 1 mL chelator (20 mM, pH 7.4) solution were combined in a 5 mL centrifuge tube and allowed to leach metals using an end-over-end rotation at 40 RPM for 24 h prior to remove undissolved solid by filtration. The resulting leachate composition was determined by ICP-OES after subjecting them to a 100-fold

dilution with 2% nitric acid (50 µL → 5000 µL). All separation experiments were repeated in duplicate.

4.2.3 Leaching kinetics

A 20 mg quantity of magnet waste or 50 mg autocat slag was contacted with ligand solution (1 mL, pH 7.4) in a 5 mL centrifuge tube, and allowed to leach metals using an end-over-end rotation at 40 RPM, and 100 µL aliquots of the supernatant were removed at different times (0.5–24 h) and filtered. The filtrates were analyzed by ICP-OES after diluting with 2% nitric acid (50 µL → 5000 µL).

Table S6. Ln^{3+} concentration in filtrates for single REE dissolution from their $REE_2(C_2O_4)_3$ using aapa. Condition: [aapa] = 5 mM, [REE^{3+}] = 5 mM, pH 4–5 (100 mM ammonium acetate buffer), [$C_2O_4^{2-}$] = 15 mM, V = 200 µL, and *t* = 1.5 h.

REE^{3+}	No L, pH 5 (µM)	1 eq. L, pH 4 (µM)	1 eq. L, pH 4.5 (µM)	1 eq. L, pH 5 (µM)
La	0.1	3532	4167	4852
Ce	0.4	3848	4487	4794
Pr	0.7	2807	4070	4425
Nd	0	2733	3706	4134
Gd	0.6	1533	3483	3939
Tb	3.9	847	3102	3888
Dy	8	548	2886	3775
Yb	0.09	286	2045	2942
Lu	0.09	272	1850	2626

Table S7. Dissolution efficiency for single REE dissolution from their $REE_2(C_2O_4)_3$ using aapa. Condition: [aapa] = 5 mM, [REE^{3+}] = 5 mM, pH 4–5 (100 mM ammonium acetate buffer), [$C_2O_4^{2-}$] = 15 mM, V = 200 µL, and *t* = 1.5 h.

REE^{3+}	No L, pH 5 (%)	1 eq. L, pH 4 (%)	1 eq. L, pH 4.5 (%)	1 eq. L, pH 5 (%)
La	0.002	70.6	83.3	97.0
Ce	0.008	77.0	89.7	95.9
Pr	0.014	56.1	81.4	88.5
Nd	0.000	54.7	74.1	82.7
Gd	0.012	30.7	69.7	78.8
Tb	0.078	16.9	62.0	77.8
Dy	0.160	11.0	57.7	75.5
Yb	0.002	5.7	40.9	58.8
Lu	0.002	5.4	37.0	52.5

Table S8. Ln^{3+} concentration in filtrates for single REE dissolution from their $REE_2(C_2O_4)_3$ using aapa. Condition: [aapa] = 5 mM, [$REE1^{3+}$] = [$REE2^{3+}$] = 2.5 mM, [$C_2O_4^{2-}$] = 15 mM, pH 4 (100 mM ammonium acetate buffer), V = 200 µL, and *t* = 1.5 h.

	La (µM)	Ce (µM)	Pr (µM)	Nd (µM)	Tb (µM)	Gd (µM)	Dy (µM)	Yb (µM)	Lu (µM)
1	1532	1585							
2	1691		1440						
3	1856			1491					
4	1907				887				
5	2025					709			
6	2017						457		
7	2065							286	
8	2088								281
9		1871	1705						
10		1875		1593					
11		1638			1162				
12		2061				867			
13		2096					392		
14		2164						352	
15		2134							306
16			1328	1382					
17			1367		1284				
18			1747			645			
19			1747				358		
20			1632					281	
21			1831						280
22				1666	1182				
23				1184		637			
24				1247			476		
25				1000				278	

26				900					160
27					1190	587			
28					1012		390		
29					713			274	
30					781				265
31						639	439		
32						489		273	
33						404			297
34							387	305	
35							400		223
36								260	207

Table S9. SF values of binary RE separation. Condition: [aapa] = 5 mM, [REE1] = [REE2] = 2.5 mM, pH 4 (100 mM ammonium acetate buffer), V = 200 μL, and *t* = 1.5 h.

SF	**Ce**	**Pr**	**Nd**	**Gd**	**Tb**	**Dy**	**Yb**	**Lu**
La	0.95	1.6	1.75	6.4	12.7	19.3	29.4	33.1
Ce		1.25	1.6	5.4	15.9	25.4	36.5	38.7
Pr			1.2	2	6.2	13.4	14.4	19.2
Nd				2.5	3	6.2	8.0	10.2
Gd					1.2	1.7	3	4.2
Tb						1.5	2	1.6
Dy							1.3	1.3
Yb								1.1

Table S10. Metal concentrations in the filtrate of magnet waste leaching. Conditions: 20 mg magnet waste. 1 mL chelator solution (20 mM); buffer: 100 mM MOPS solution (pH 7.4); *t* = 24 h, rotated at 40 rpm. REEs are highlighted in green and the most significant non-REEs are highlighted in orange cells.

	4 M HNO_3 (ppm)	Aapa (ppm)	Macropa (ppm)	DTPA (ppm)	Water (ppm)
Pr	19.4	8.0	8.0	4.9	-0.1
Nd	2132.4	828.3	819.4	520.8	-0.2
Dy	107.5	41.6	29.4	24.0	0.0
Mg	23.9	7.6	14.3	0.7	0.7
Al	1542.1	17.4	10.3	36.4	14.3
Fe	6244.4	179.3	57.8	342.0	0.5
Ca	75.7	14.3	17.5	4.6	-1.3
Ba	193.9	112.8	112.0	0.5	0.0
Cu	2829.9	120.6	265.9	363.2	0.0
Ni	620.2	11.8	8.4	15.3	-0.6
Zn	141	51.6	59.7	71.7	0.1
Total	13930.4	1393.3	1402.7	1384.1	-

Table S11. Metal percentage in the filtrate of magnet waste leaching. Conditions: 20 mg magnet waste. 1 mL chelator solution (20 mM); buffer: 100 mM MOPS solution (pH 7.4); *t* = 24 h, rotated at 40 rpm. REEs are highlighted in green and the most significant non-REEs are highlighted in orange cells.

REE	4 M HNO_3 (%)	Aapa (%)	Macropa (%)	DTPA (%)
Pr	0.1	0.6	0.6	0.4
Nd	15.3	59.4	58.4	37.6
Dy	0.8	3.0	2.1	1.7
Mg	0.2	0.5	1.0	0.1
Al	11.1	1.2	0.7	2.6
Fe	44.8	12.9	4.1	24.7
Ca	0.5	1.0	1.2	0.3
Ba	1.4	8.1	8.0	0.0
Cu	20.3	8.7	19.0	26.2
Ni	4.5	0.8	0.6	1.1
Zn	1.0	3.7	4.3	5.2
Total	100	100	100	100

Table S12. Pulp density optimization of **aapa** for autocat slag. Conditions: 10–50 mg autocat slag. 1 mL aapa (20 mM); buffer: 100 mM MOPS solution (pH 7.4); *t* = 24 h, rotated at 40 rpm. REEs are highlighted in green and the most significant non-REEs are highlighted in orange cells.

Elements	10 g/L	20 g/L	30 g/L	40 g/L	50 g/L
La	1.8	2.6	3.4	3.7	3.8
Ce	12.4	17.8	22.5	26.4	28.4
Pr	0.5	0.6	0.8	0.9	0.9
Nd	1.1	1.5	1.9	2.1	2.3
Ba	1.0	1.6	2.2	2.6	3.0
Sr	0.4	0.7	1.0	1.2	1.4
Mg	5.7	10.7	15.7	18.9	21.8
Al	5.7	8.4	11.2	12.4	13.3
Fe	6.7	11.4	17.1	19.2	21.2
Ca	19.0	33.4	54.7	66.7	78.9

Figure S13. Pulp density optimization of **macropa** for autocat slag. Conditions: 10–50 mg autocat slag. 1 mL aapa (20 mM); buffer: 100 mM MOPS solution (pH 7.4); *t* = 24 h, rotated at 40 rpm. REEs are highlighted in green and the most significant non-REEs are highlighted in orange cells.

Elements	10 g/L	20 g/L	30 g/L	40 g/L	50 g/L
La	0.4	0.7	1.0	1.3	1.6
Ce	2.4	4.5	6.2	8.1	10.2
Pr	0.1	0.2	0.2	0.3	0.3
Nd	0.2	0.4	0.5	0.7	0.8
Ba	0.7	1.2	1.6	2.0	3.0
Sr	0.3	0.5	0.8	1.0	1.0
Mg	4.8	9.2	13.0	17.0	19.2
Al	0.7	0.7	0.9	1.1	1.7
Fe	3.9	8.5	11.1	15.5	21.2
Ca	15.9	32.2	43.5	60.0	75.9

Table S14. Metal concentrations in the filtrate of autocat slag leaching. Conditions: 50 mg autocat slag. 1 mL chelator solution (20 mM); buffer: 100 mM MOPS solution (pH 7.4); *t* = 24 h, rotated at 40 rpm. REEs are highlighted in green and the most significant non-REEs are highlighted in orange cells.

	4 M HNO_3 (ppm)	Aapa (ppm)	Macropa (ppm)	DTPA (ppm)	Water (ppm)
La	169.9	3.8	1.6	4.9	-0.1
Ce	1143.3	28.4	10.2	33.1	-0.4
Pr	230.6	0.9	0.3	6.6	-0.2
Nd	89.5	2.3	0.8	2.4	-0.2
Ba	246.2	3.0	3.0	1.1	-0.2
Sr	67.2	1.4	1.0	1.0	0.1
Mg	687.8	21.8	19.2	11.4	0.5
Al	3708.5	13.3	1.7	18.5	3.2
Fe	1091.5	28.0	21.2	50.3	0.2
Ca	5857.7	78.9	75.9	125.4	4.7

Table S15. Metal percentage in the filtrate of autocat slag leaching. Conditions: 50 mg autocat slag. 1 mL chelator solution (20 mM); buffer: 100 mM MOPS solution (pH 7.4); *t* = 24 h, rotated at 40 rpm. REEs are highlighted in green and the most significant non-REEs are highlighted in orange cells.

REE	4 M HNO_3 (%)	Aapa (%)	Macropa (%)	DTPA (%)
La	1.3	2.1	1.2	1.9
Ce	8.6	15.6	7.6	13.0
Pr	1.7	0.5	0.2	2.6
Nd	0.7	1.3	0.6	0.9
Ba	1.9	1.6	2.2	0.4
Sr	0.5	0.8	0.7	0.4
Mg	5.2	12.0	14.2	4.5
Al	27.9	7.3	1.3	7.3
Fe	8.2	43.4	56.2	49.2
Ca	44.1	15.4	15.7	19.7
Total	100	100	100	100

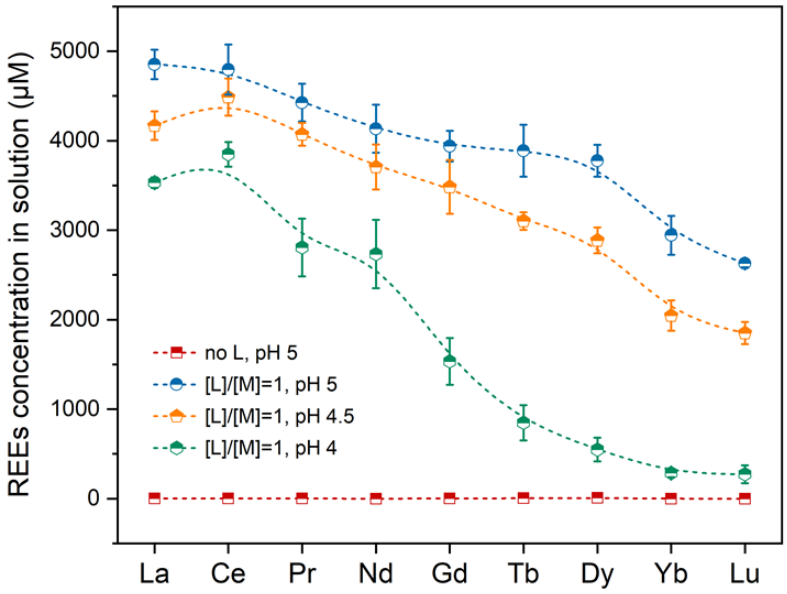

Figure S45. Soluble REE concentration within the filtrate determined by ICP-OES for single $REE_2(C_2O_4)_3$ in the absence of aapa and in the presence of aapa at different pH values. Conditions: $[REE^{3+}]$ = 5 mM, $[C_2O_4^{2-}]$ = 15 mM, [aapa] = 5 mM; buffer: 100 mM ammonium acetate; *t* = 1.5 h.

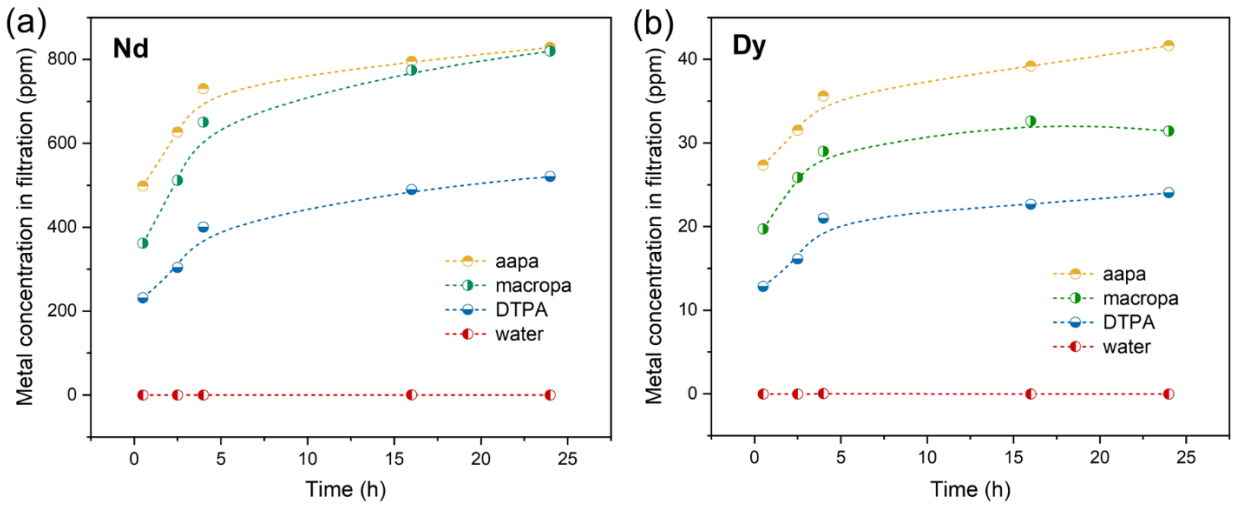

Figure S46. Leaching kinetics of aapa for Nd^{3+} and Dy^{3+} from magnet waste. Conditions: 20 mg magnet waste. 1 mL chelator solution (20 mM); buffer: 100 mM MOPS solution (pH 7.4); *t* = 0.5–24 h, rotated at 40 rpm.

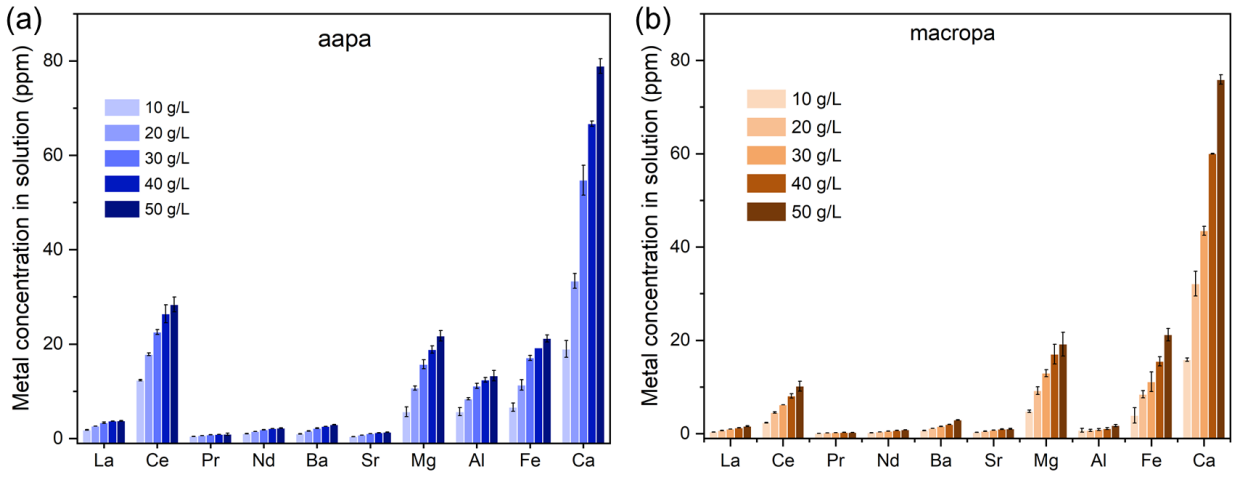

Figure S47. The optimization of pulp density for autocat slag. Conditions: 10–50 mg autocat slag. 1 mL chelator solution (20 mM); buffer: 100 mM MOPS solution (pH 7.4); *t* = 24 h, rotated at 40 rpm.

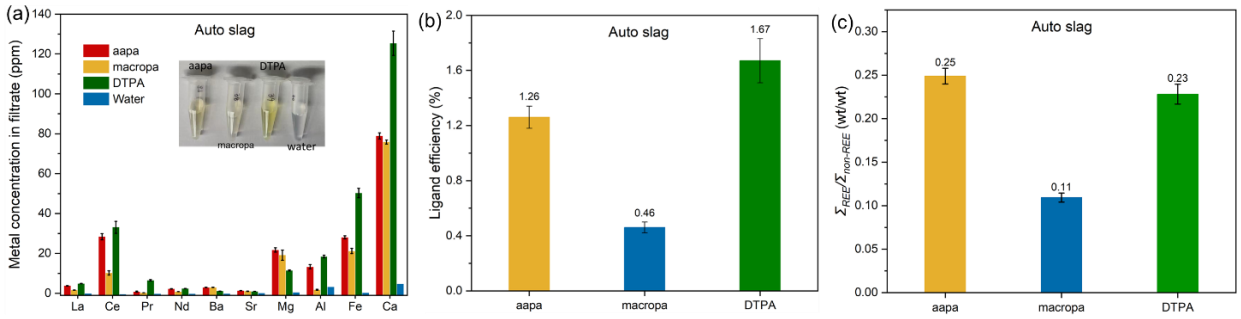

Figure S48. REEs leaching from autocat slag using different chelators. (a) Metal concentration in the filtrate of autocat slag leaching; (b) Ligand efficiency of REEs for autocat slag; (c) Weight ratio of REE to non-REEs in the filtrate of autocat slag leaching. Conditions: 50 mg autocat slag. 1 mL chelator solution (20 mM); buffer: 100 mM MOPS solution (pH 7.4); *t* = 24 h, rotated at 40 rpm.

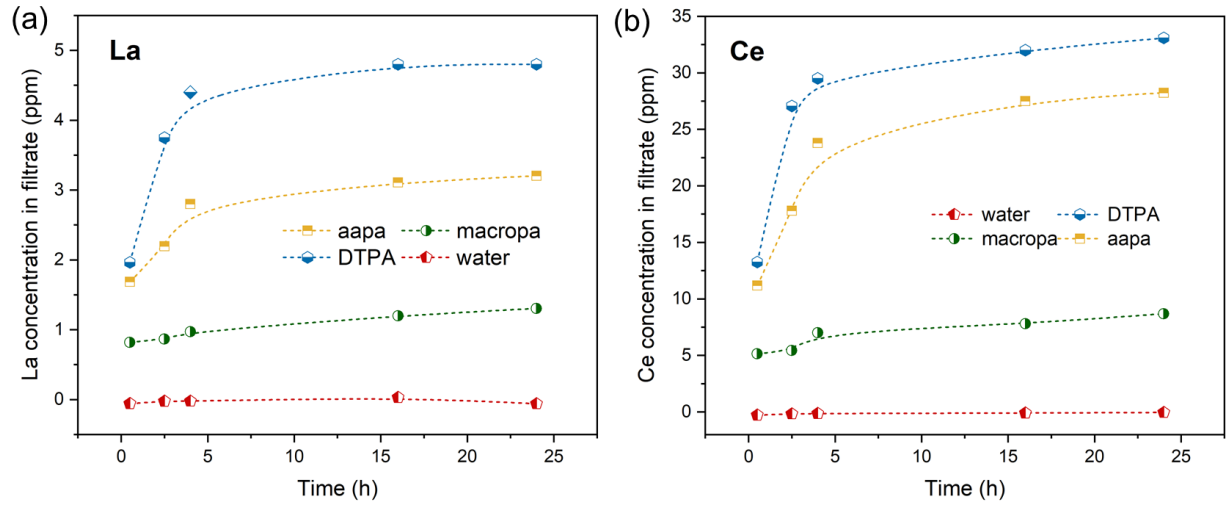

Figure S49. Leaching kinetics of aapa for La^{3+} and Ce^{3+} from autocat slag. Conditions: 50 mg autocat slag. 1 mL chelator solution (20 mM); buffer: 100 mM MOPS solution (pH 7.4); t =0.5–24 h, rotated at 40 rpm.

References

(1) Woods, J. J.; Unnerstall, R.; Hasson, A.; Abou, D. S.; Radchenko, V.; Thorek, D. L. J.; Wilson, J. J. Stable Chelation of the Uranyl Ion by Acyclic Hexadentate Ligands: Potential Applications for 230U Targeted α-Therapy. *Inorg. Chem.* **2022**, *61* (7), 3337–3350. https://doi.org/10.1021/acs.inorgchem.1c03972.

(2) CrysAlisPro. Rigaku OD. CrysAlisPro: The Woodlands 2015.

(3) George M. Sheldrick. A Short History of SHELX. *Acta Crystallographica Section A* **2008**, *64* (1), 112–122.

(4) Peter Müller. Practical Suggestions for Better Crystal Structures. *Crystallography Reviews* **2009**, *15*, 57–83.

(5) George M. Sheldrick. SHELXT – Integrated Space-Group and Crystal-Structure Determination. *Acta Crystallogr. Sect.* **2015**, *71* (1), 3–8.

(6) Sweeton, F. H.; Mesmer, R. E.; Baes, C. F. Acidity Measurements at Elevated Temperatures. VII. Dissociation of Water. *J. Solution Chem.* **1974**, *3* (3), 191–213.

(7) Gran, G. Determination of the Equivalent Point in Potentiometric Titrations. *Acta Chemica Scandinavic* **1950**, *4*, 559–577.

(8) Wuhan University. *Analytical Chemistry I, 5th Ed.; Higher Education Press: Beijing,*; 2006.

(9) Garw, P.; Sabatinib, A.; Vaccab, A. Investigation of Equilibria in Solution. Determination of Equilibrium Constants with the HYPERQUAD Suite of Programs. *Talanta* **1996**, *43*, 1739–1753.

(10) Gans P., Sabatini. A. Vacca A. Determination of Equilibrium Constants from Spectrophometric Data Obtained from Solution of Known PH: The Program pHab. *Ann. Chim.* **1999**, *89*, 45–49.

(11) Nelson, J. J. M.; Cheisson, T.; Rugh, H. J.; Gau, M. R.; Carroll, P. J.; Schelter, E. J. High-Throughput Screening for Discovery of Benchtop Separations Systems for Selected Rare Earth Elements. *Commun. Chem.* **2020**, *3*, 7. https://doi.org/10.1038/s42004-019-0253-x.